 https://doi.org/10.3311/PPci.20220

Periodica Polytechnica Civil Engineering, 66(3), pp. 900–921, 2022

Chaotically Enhanced Meta-Heuristic Algorithms for Optimal Design of Truss Structures with Frequency Constraints

Ali Kaveh[1*], Hosein Yosefpoor[2]

[1] Department of Civil Engineering, Iran University of Science and Technology, Narmak, 1684613114 Tehran, Iran
[2] Department of Civil Engineering, Science and Research Branch, Islamic Azad University, 1477893855 Tehran, Iran
[*] Corresponding author, e-mail: alikaveh@iust.ac.ir

Received: 24 March 2021, Accepted: 03 May 2022, Published online: 19 May 2022

Abstract

The natural frequencies of any structure contain useful information about the dynamic behavior of that structure, and by controlling these frequencies, the destructive effects of dynamic loads, including the resonance phenomenon, can be minimized. Truss optimization by applying dynamic constraints has been widely welcomed by researchers in recent decades and has been presented as a challenging topic. The main reason for this choice is quick access to dynamic information by examining natural frequencies. Also, frequency constraint relations are highly nonlinear and non-convex and have implicit variables, so using mathematical and derivative methods will be very difficult and time consuming. In this regard, the use of meta-heuristic algorithms in truss weight optimization with frequency constraints has good results, but with the introduction of form variables, these algorithms trap at local optima. In this research, by applying chaos map in meta-heuristic algorithms, suitable conditions have been provided to escape from local optima and access to global optimums. These algorithms include Chaotic Cyclical Parthenogenesis Algorithms (CCPA), Chaotic Biogeography-Based Optimization (CBBO), Chaotic Teaching-Learning-Based Optimization (CTLBO) and Chaotic Particle Swarm Optimization (CPSO), respectively. Also, by using different scenarios, a good balance has been achieved between the exploration and exploitation of the algorithms.

Keywords

frequency constraints, shape and cross section optimization, meta-heuristic algorithms, chaos map

1 Introduction

Due to the diversity in the use of truss structures, the optimization of these structures has received more and more attention of the researchers. If these structures are selected to cover large openings, they will have a large number of members, and if used as telecommunication and transmission towers, they will usually be built in large numbers. Therefore, by optimizing this type of structures, resources and costs are significantly saved. For this reason, variables related to cost and efficiency along with engineering criteria such as strength and stability are considered. In most cases, the weight index is the main goal of the optimization, but in cases where structures are affected by dynamic loads such as earthquakes and storms, to prevent resonance, their natural frequency should be limited to a certain range. To apply this type of constraint, the natural frequencies of the structures contain all the necessary information about the dynamic behavior of the structures. In low frequency vibration problems, the response of the structure depends on the base frequencies and the modal shape, and by applying a frequency limit, the dynamic behavior of the structure is easily controlled. In a number of optimization problems, by applying these relationships, the effects of some modes can be reduced. For example, in the design of aircraft wings, efforts are made to reduce bending and torsional modes. The design variables related to the cross section of the members are not explicitly present in the dynamic equations of the structures and their presence is implicit, so if optimization is done with mathematical methods and implicit derivatives, we will encounter strongly "nonlinear and non-convex equations that solve them." It will be very difficult and time consuming. Consequently, if we want to solve frequency constraints in an optimization using traditional methods, we must perform a sensitivity analysis. Derivatives of the eigenvalues and eigenvectors must therefore be calculated, and this will usually require some kind of approximation. In addition,

Cite this article as: Kaveh, A., Yosefpoor, H. "Chaotically Enhanced Meta-Heuristic Algorithms for Optimal Design of Truss Structures with Frequency Constraints", Periodica Polytechnica Civil Engineering, 66(3), pp. 900–921, 2022. https://doi.org/10.3311/PPci.20220

in some cases due to symmetry we will encounter repetitive eigenvalues and repetitive frequencies that are indistinguishable from ordinary studies and can only be determined with directional derivatives. When analyzing the sensitivity of structures, a certain complexity is created by the repetitive frequencies, mainly because the eigenvalues are not unique. Another limitation that greatly affects the traditional methods of mathematical optimization is the choice of a good starting point. In cases where the selected starting point is not appropriate, these methods are stopped when reaching the local optima, and no solution is provided to escape from these local optima. Today, with the complexity of issues and the increase in the number of decision variables, the unresponsiveness of classical methods becomes evident. Therefore, in order to overcome these challenges in the last decade, various types of powerful optimization methods have been developed, in some of which the optimization of structures with frequency constraints has been considered. Most of these optimization methods are inspired by meta-heuristic techniques. Meta-heuristic algorithms have been widely welcomed by researchers and are powerful tools for engineering optimization problems. The main features of these methods can be expressed in the following cases:

They are based on the population. They are independent of the specific issue. They are inspired by natural phenomena. They do not need any gradient information of objective function and constraints. The quality of the final solution does not depend on the starting point. They are based on decisions and principles of random search. In these algorithms, the value of the objective function itself is used instead of derivatives and they have global search capabilities. Meta-heuristics are also suitable for complex, nonlinear, discrete and non-convex search spaces [1]. In the classification of these algorithms, the source of inspiration has played an important role. Some of these sources of inspiration consist of algorithms based on evolution and evolution, algorithms based on collective intelligence, algorithms based on physical laws, algorithms based on environment and algorithms based on social and human laws. We introduce examples for each of these groups. Genetic Algorithms (GA) [2–3], Evolutionary Strategy (ES) [4] and Differential Evolution (DE) [5] are inspired by evolution. Cyclical Parthenogenesis Algorithms (CPA) [6], Particle Swarm Optimization (PSO) [7–8], Artificial Bee Colony (ABC) [9], Cuckoo Search (CS) [10], Ant Colony Optimization (ACO) [11], Gray Wolf Optimization (GWO) [12–13] and Whale Optimization Algorithm (WOA) [14] Inspired by swarming intelligence. Optimization algorithms based on water Evaporation Optimization (WEO) [15–16], Charged System Search (CSS) [17], Colliding Bodies Optimization (CBO) [18–20], Vibrating Particles System (VPS) [21–22], Thermal Exchange Optimization (TEO) [23], Big Bang-Big Crunch (BB-BC) [24–25], Ray Optimization (RO) [26–27] and Harmony Search (HS) [28] are inspired by the laws of physics. Also, Biogeography-Based Optimization (BBO) [29], Teaching-Learning-Based Optimization (TLBO) [30], Imperialist Competitive Algorithm (ICA) [31] and Shuffled Frog-Leaping Algorithm (SFLA) [32] are among the algorithms inspired by the environment, social and human laws and behavior, respectively. In each of these algorithms, a number of random numbers are involved that we use the system of alternative turbulence functions to improve the escape conditions from local optima. Mathematically, chaos refers to the ability of a simple pattern and model to show virtually no signs of random phenomena, but to lead to the emergence of disordered reaction behaviors in the environment. The salient features of a chaotic system are: 1) They are sensitive to initial conditions. 2) Their alternating rotation is dense. 3) They have quasi-random and non-periodic behavior. At present, these dynamic systems are considered by many scientific societies and in various scientific disciplines such as engineering, medicine, biology and economics, the amazing effects of its use are observed. The term butterfly effect was suggested following an article by Edward Lawrence. At the 39th World Water Summit, Lawrence presented an article entitled: "Can a butterfly fly in Brazil cause strong winds in Texas?" [33]. Research shows that using chaos map instead of random distribution functions has yielded very valuable results. In structural optimization applications, some of these turbulence functions are very likely to converge from a local minimum to a general minimum, and can make significant improvements to meta-exploration algorithms with poor search performance. In some other turbulence functions, unlike the previous case, the probability of being present in the range of local minima is higher and for algorithms that have poor extraction, a significant improvement is observed. Therefore, in this research, samples are selected from each of the groups of chaos map and applied with different scenarios in meta-heuristic algorithms. Optimization algorithms include cyclic fertilization algorithm, biogeography based algorithm, teaching and learning based algorithm and particle swarm optimization algorithm. These

algorithms are combined with Gaussian, Liebovitch and Piecewise chaos map with different scenarios. In most cases, the placement of chaos map in the meta-heuristic algorithms has a significant improvement. This becomes evident from the comparison of the combined modes with the standard modes. In the following sections, this type of enhancement is investigated.

2 Natural frequencies and formulation of optimization problems

In this group of optimization problems, first the calculation of natural frequencies of the structure is examined and then the formulation of optimization problems with limitation of vibrational frequencies is presented. To calculate the natural frequencies of the structure, the matrix form of the free vibration equation is a system of several degrees of freedom according to Eq. (1). In this equation, M represents the mass matrix, K the stiffness matrix, and Y is the displacement equation. To facilitate the solution of the equation, $\boldsymbol{\varphi}_n$ of the nth modal shape vector and $q_n(t)$ of the nth modem time curve are separated and the results are formed according to Eqs. (2) to (4). The values of A_n and B_n are integral constants that are determined from the initial conditions of velocity and displacement. Now, to determine the natural frequencies and deformation modes (ω_n and φ_n), by placing $Y(t)$ in the equation of free vibration, Eq. (5) is obtained. The roots of this characteristic equation are known as eigenvalues of frequencies.

$$\boldsymbol{M}\times\ddot{Y}(t)+\boldsymbol{K}\times Y(t)=0 \tag{1}$$

$$Y(t)=\boldsymbol{\Phi}_n\times q_n(t);\quad n=1,2,...,N \tag{2}$$

$$q_n(t)=A_n\cos\omega_n t+B_n\sin\omega_n t \tag{3}$$

$$Y(t)=\boldsymbol{\Phi}_n\times(A_n\cos\omega_n t+B_n\sin\omega_n t) \tag{4}$$

$$\left[\boldsymbol{K}-\omega_n^2\times\boldsymbol{M}\right]\times\boldsymbol{\Phi}_n=0\quad\Rightarrow\quad\left|\boldsymbol{K}-\omega_n^2\times\boldsymbol{M}\right|=0 \tag{5}$$

By expanding the determinant, the number N is the real and positive root for $\omega_n{}^2$, which contains the natural frequencies of the structure. In optimization problems for the cross section and geometric shape of trusses that are associated with frequency constraints, the goal is to minimize the weight of the structure so that the constraints for a number of natural frequencies for vibration modes are satisfied. The cross section of the members along with the coordinates of some nodes are introduced as decision variables. These variables are selected continuously. The upper and lower bounds are also specified for variables in some cases. These optimization problems are defined in mathematical form according to Eq. (6):

$$\begin{aligned}&Find\quad X=\{A,S\},\quad A=\{A_1,A_2,...,A_{na}\},S=\{S_1,S_2,...,S_{ns}\}\\&to\ Minimize:\ W(A,S)=\sum_{i=1}^{nm}\rho_i\times L_i(S)\times A_i\\&subjected\ to:\begin{cases}\tilde{\omega}_i^L\le\omega_i\le\tilde{\omega}_i^U & i=1,2,...,n\omega\\ A_j^L\le A_j\le A_j^U & j=1,2,...,na.\\ S_k^L\le S_k\le S_k^U & k=1,2,...,ns\end{cases}\end{aligned} \tag{6}$$

In this relation, $\boldsymbol{X}$ is the vector of decision variables, A is the variable of the cross-section of the members, na represents the number of variables of the cross-section, A_i is the value of the cross-section of the ith variable, S is the variable of shape and arrangement, ns is the number of shape variables with the same coordinates. S_i is the numerical value of the ith variable, W expresses the weight of the truss, nm indicates the total number of members, ρ_i the specific gravity of the material belonging to the ith member of the truss, L_i the length corresponding to the ith member which can be expressed through the variables, ω_i expression of the ith natural frequency of the truss, ω_i^L and ω_i^u, respectively, represent the lower limit and the upper limit of the fixed frequency of the base, $n\omega$ indicates the total number of frequency restrictions, Aj^L and Aj^u, respectively, express the lower limit and the upper limit of the Aj cross section, and S_k^L and S_k^U show the lower limit and limit of kth variable S_k. Then meta-heuristic algorithms are used for unbounded problems; we use the penalty function in modeling to convert the bounded state to unbounded state. In this method, if no violation has been committed, the amount of the fine will be zero, otherwise, if there is a violation, the amount of the penalty function will be obtained from Eqs. (7) to (10):

$$V_i=\begin{cases}0 & if\quad\tilde{\omega}_i^L\le\omega_i\le\tilde{\omega}_i^U\\ 1-\dfrac{\omega_i}{\tilde{\omega}_i^L} & if\quad\tilde{\omega}_i^L>\omega_i\\ 1-\dfrac{\tilde{\omega}_i^U}{\omega_i} & if\quad\omega_i>\tilde{\omega}_i^U\end{cases}, \tag{7}$$

$$\gamma=\sum_{i=1}^{n\omega}V_i, \tag{8}$$

$$F_{penalty}=(1+\varepsilon_1\times\gamma)^{\varepsilon_2}, \tag{9}$$

$$to\ Minimize\quad Mer(A,S)=W(A,S)\times F_{penalty}. \tag{10}$$

In these relations γ represents the set of violations and ε_1 and ε_2 are selected based on the search and extraction ratio. In this study, ε_1 units and ε_2 are selected with incremental linear changes in the range of 1.3 to 3 at the end of the iteration. Finally, *Mer* is the merit function or the objective function after the penalty is imposed.

3 Introduction chaos maps and forming chaos series

In most meta-heuristic algorithms, the optimization results stagnate and stop when they reach the local optimal position. In such cases, premature convergence occurs. In order to escape from the trap of local optima, chaos series create suitable conditions that by creating disorder in the search space, the possibility of jumping and settling in most scattered positions of the search space is implemented. Therefore, the general optima will not have the opportunity to escape from their target. How to apply them to meta-exploration algorithms is shown in the flowchart of Fig. 1. Chaos series consists of the arrangement of chaotic function sentences. These series have no traces of random behaviors, but they cause very disordered behaviors in the search space. One of the most important features of these series is sensitivity to initial conditions and non-periodic and ergodic behaviors, and the functions that make up the chaos series are very diverse and have no inverse [34].

In this research, Gaussian, Liebovitch and Piecewise chaos maps have been selected to form chaos series. In the chaos maps, Liebovitch converges with a very high probability from a local minimum to a general minimum. Therefore, this map is suitable for improving the exploration conditions of algorithms. The chaos Gaussian map is most likely in the local minimum range and is suitable for improving exploitation conditions. Finally, the chaotic map of Piecewise simultaneously improves both exploration and exploitation conditions. Therefore, by selecting these chaotic functions, the weakness of algorithms of any kind is improved. The numerical distribution of these chaos maps for 100 iterations is presented in Fig. 2. In the following, we will first introduce chaos functions and then chaos series to form chaos scenarios are presented.

3.1 Gaussian map

Using this function in nonlinear dynamic behaviors has good results [35]. The statements of chaotic sequences in the Gaussian function are obtained according to the Eq. (11):

$$X_{n+1} = \begin{cases} 0 & X_n = 0 \\ \frac{1}{X_n} - \left[\frac{1}{X_n}\right] & X_n \neq 0 \end{cases}. \tag{11}$$

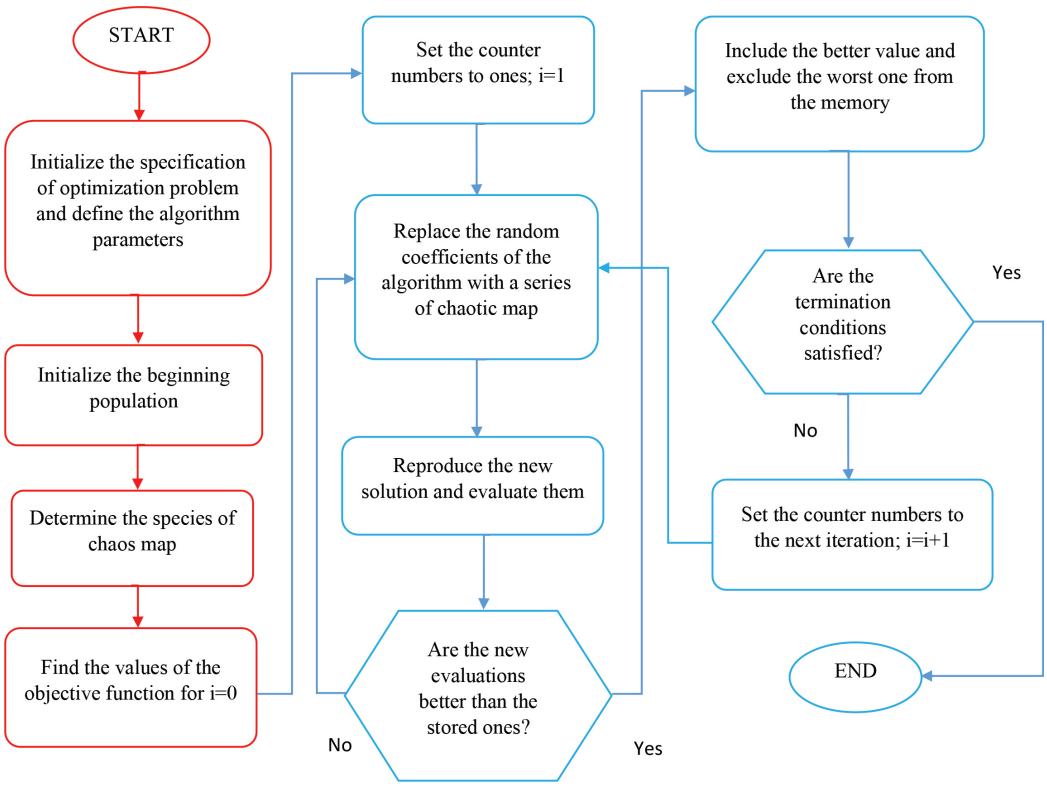

Fig. 1 Flowchart of applying chaos functions to meta-heuristic algorithms

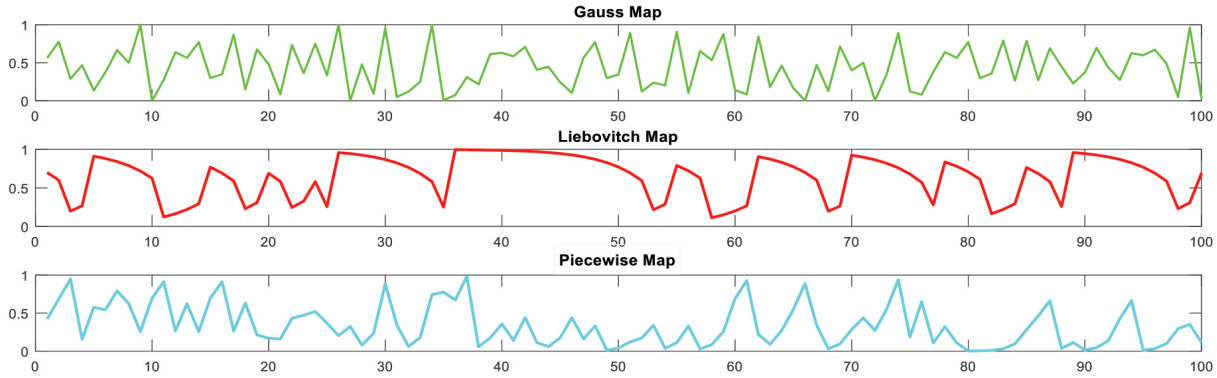

Fig. 2 Distribution of numerical values of chaos functions in 100 repetitions

3.2 Liebovitch map

This function consists of three separate linear rules and there will be no common or repetitive sentences in these intervals [36]. The chaotic sequence sentences in this function are expressed by the Eq. (12):

$$X_{n+1}=\begin{cases}\alpha_1 X_n & 0<X_n\le d_1\\ \dfrac{d_2-X_n}{d_2-d_1}: & d_1<X_n\le d_2\\ 1-\alpha_2\times(1-X_n) & d_2<X_n\le 1\end{cases}. \tag{12}$$

Here the values $d_1 = 1/3$ and $d_2 = 2/3$ are selected. A_1 and α_2 are also calculated based on the Eqs. (13) and (14):

$$\alpha_1=\frac{d_2}{d_1}\times(1-(d_2-d_1)) \tag{13}$$

$$\alpha_2=\frac{1}{d_2-1}((d_2-1)-d_1(d_2-d_1)) \tag{14}$$

3.3 Piecewise map

The piecewise map is the same as the Liebovitch map of three criteria, and the value of P is considered as the control parameter [33]. The range of changes of P is in the range of 0 to 0.5, which in this study we have considered 1/3, and the following category of equations indicates the relationship between the sentences of chaotic sequences in this function that expressed by the Eq. (15):

$$X_{n+1}=\begin{cases}\dfrac{X_n}{p} & 0\le X_n<p\\ \dfrac{X_n-p}{0.5-p} & p\le X_n<\dfrac{1}{2}\\ \dfrac{1-p-X_n}{0.5-p} & \dfrac{1}{2}\le X_n<1-p\\ \dfrac{1-X_n}{p} & 1-p\le X_n<1\end{cases} \tag{15}$$

3.4 Chaos series and alternative scenarios

By selecting the chaos maps, two groups of chaos series **CHM1** and **CHM2** are formed and replace the probable parameters of the meta-heuristic algorithms according to the required number of sentences. **CHM1** chaotic series sentences are related to the first scenario and replace the probable parameters related to the exploration stage, the sentences of the **CHM2** chaos series are related to the second scenario and will replace the probable parameters related to the exploitation stage, and finally, for the third scenario, the simultaneous application of the **CHM1** and **CHM2** chaos series in both the exploration and exploitation stages will be considered.

4 Meta-heuristic algorithms and chaos map

Each meta-heuristic algorithm goes through two main stages of exploration and exploitation in the optimization stages to converge towards the optimal answers. In other words, it first settles in scattered parts of the search space and then examines their neighborhood. For example, in the Genetic Algorithm, in the stage of mutation, the establishment takes place in scattered areas of the search space, and in the stage of crossover, in the neighborhood, the movement towards better answers takes place. Correspondingly, in the Imperialist Competitive Algorithm, settling in different parts of the search space with the action of revolution and moving in the neighborhood towards better answers will be done with the policy of assimilation. In each of these two stages, random coefficients are predicted to create diversity in the search space and their values are recommended based on a specific probabilistic distribution. In some meta-heuristic algorithms, uniform probabilistic distribution is used, which naturally would not be a good distribution, but a Normal or Cauchy distribution, is associated with admirable results. Especially the normal distribution has a very wide range and creates a good diversity.

Since the random selection has always been accompanied by doubt, the idea of using chaos maps that their values are definite and alternatives are good for random distributions. Scientific studies have recorded valuable results and significant improvements for them. Chaos systems can provide an inclination towards global responses and have the potential to prevent them from falling into the trap of local optima. If these conditions are met, one will no longer see premature convergence. Lorenz points out the following important points about series formed by chaos maps: Although series created by chaotic functions appear to be similar to sentences with random distributions, there are major differences. Some of these differences are: their values are deterministic, they have nonlinear behavior, they are dynamic state, the sentences of the series related to them are non-repetitive, most of them have no inverse functions and finally non-convergent to a certain boundary [33]. Now, by replacing chaos series in meta-heuristic algorithms, the nonlinear and non-convex behavior of the objective function in truss weight optimization can be easily controlled and adjusted by them. In this research, in order to investigate the effects of chaos series in improving the optimization results of algorithms, by selecting four meta- heuristic algorithms, a wide range of chaotic modes have been formed and challenging competition has been obtained. The selection of meta- heuristic algorithms is such that the standard mode of the algorithm has excellent efficiency in at least one of the exploration or exploitation cases to compensate for the weakness related to the other case by chaotic series. These algorithms include Chaotic Cyclical Parthenogenesis Algorithms (CCPA), Chaotic Biogeography-Based Optimization (CBBO), Chaotic Teaching-Learning-Based Optimization (CTLBO) and Chaotic Particle Swarm Optimization (CPSO), respectively. Each standard state is compared with 9 chaotic states. Therefore, the final optimal state is selected from forty optimization designs with different methods and inspirations. Due to the wide statistical space to introduce the optimal design, we will have intensive challenge and competition for the desire for absolute optimality. Therefore, the possibility of accessing optimal global responses with high accuracy has increased. Other important results in this research can be the introduction of the best algorithm, the best chaotic function and the best scenario. In the following studies, we will introduce each of the algorithms in standard and chaotic mode.

4.1 Standard cyclical Parthenogenesis algorithm (CPA)

The idea of this algorithm was presented by Kaveh and Zolghadr [6] and it has significantly improved the shape and cross section of structures with frequency constraints. In this algorithm, the key aspects of aphids' life are discussed. Their ability to reproduce sexually and asexually provides the conditions for the rapidly growing population of aphids to form and take advantage of favorable conditions. Research shows that in sexual reproduction, two different solutions share information, while in asexual reproduction, the new solution is produced solely using the information of a female parent. Applying this inspiration to meta-heuristic algorithms creates the best conditions for balancing between exploration and exploitation, and provides a high capability for escaping local optimization and moving toward global optimization. In the sexual reproduction stage, the initial response vector is located in scattered areas of the search space, and in the asexual reproduction stage, the neighborhood carefully examines the resulting responses. Therefore, general answers cannot be far from the scope of this algorithm.

4.1.1 Basic steps of cyclical parthenogenesis algorithm

Step 1. Creating an initial population of aphids: Within the search space, a population of aphids is formed as the primary population. The selection of this population is random. In the following relation, the method of selecting the initial population is presented from Eq. (16):

$$x_{ij}^{0} = x_{j,\min} + rand \times (x_{j,\max} - x_{j,\min}) \quad i = 1,2,...,nA, \quad j = 1,2,...,n\,\text{var} \tag{16}$$

Where $x_{ij}^{\ 0}$ denotes the *j*th variable of the *i*th population of aphids, $x_{j,\max}$ and $x_{j,\min}$, respectively expresses the upper and lower bounds of the variable *j*. The total population of aphids is *nA*, which are located in colonies with *nC* number and each with *nM* population. It is clear that *nM* = *nA*/*nC* and *nM* is constant during the optimization operation.

Step 2. Formation of the population of children: To form the population of offspring in each colony, the number of *Fr* × *nM* offspring without mating is formed. The parents of these children are female, and their selection is done randomly and from the best answers. In MATLAB coding, this selection and formation of the children population is as Eqs. (17) and (18).

$$rf_i = round(1 + (Fr \times nM - 1). \times \mathbf{rand}) \tag{17}$$

$$x_{ij}^{k+1} = F_j^k + \alpha_1 \times \frac{randn}{NITs} \times (x_{j,\max} - x_{j,\min}) \quad j = 1,2,...,n\,\text{var} \tag{18}$$

In relation to Eq. (17), the index related to the female parent is determined and in relation to (18) new children related to the state without mating, it is placed in the new cell array. Now it is time to form offspring by mating. The number of these offspring is (1–*Fr*)*xnM* in which each male parent *M* randomly selects a female parent *F* and is placed in a new cell array according to the relationship of the Eq. (19) new children related to mating.

$$x_{ij}^{k+1} = M_j^k + \alpha_2 \times \mathbf{rand} \times (F_j^k - M_j^k) \quad j = 1,2,...,n \text{ var} \tag{19}$$

Step 3. Fly the best aphid and death to the worst aphid: After the formation of a new generation of offspring, the target function is evaluated and with a probability of *Pf*, one of the best winged aphid is selected from colony 1 and by reproducing it, it replaces the worst aphid in colony 2. To keep the colony population stable, removing the worst colony 2 aphid is compared to the death of the aphid and replacing the best aphid with flying. The probability of this step is based on Eq. (20):

$$pf = \frac{NITs - 1}{\max NITs - 1} \tag{20}$$

Step 4. Replacing the best aphid: In each colony, the population of parents is compared with that of children, and the number of *nM* from the best is selected to form the next generation.

Step 5. Check the terminating conditions and repeat the operation from step 2 if necessary.

4.1.2 Chaotic enhanced cyclical parthenogenesis algorithm (CCPA)

In this algorithm, two important modes are selected to form the population of offspring, including reproduction with and without mating. These two steps have the role of exploration and exploitation of the algorithm. By replacing chaos maps instead of random selection, one will have a significant improvement in optimization results. This replacement is done with the following proposed scenarios:

Scenario 1. Apply the chaos map in reproduction stage without mating: In this case, the first chaos map **CHM1** is applied in Eq. (17) and replaces the random selection of the algorithm that the result will be Eq. (21):

$$rf_i = round(1 + (Fr \times nM - 1) \times \mathbf{CHM1}) . \tag{21}$$

Scenario 2. Apply the chaos map in reproduction stage with mating: In this case, the second chaos map **CHM2** is applied in Eq. (19) and replace the random selection of the algorithm that the result will be Eq. (22):

$$x_{ij}^{k+1} = M_j^k + \alpha_2 \times \mathbf{CHM2} \times (F_j^k - M_j^k) \quad j = 1,2,...,n \text{ var} \tag{22}$$

Scenario 3. Apply the chaos maps in both steps simultaneously: In this case, both chaos maps are applied simultaneously in Eqs. (17) and (19) and replace the random selection of the algorithm.

4.2 Standard biogeography-based optimization (BBO)

The idea for this algorithm was proposed in 2008 by Simon [29]. This algorithm examines the distribution of plant and animal species in different geographical habitats. The monopoly of animals and plants in the possession of food resources, water, etc. are their main goals, but due to the limitation of these resources, they will be forced to share it with each other. In the process, an ecosystem emerges from which species feed on other species. Examination of the population distribution of habitats indicates the fact that animals prefer to migrate to more secluded places and if the settlement is less populated, it will be a suitable place for migration. On the other hand, areas with better food sources will naturally have more population. In this regard, the HSI habitat competency factor will affect the choice of location. In engineering optimization problems, this coefficient plays the role of the objective function of the problem. In comparison between habitats, the high of this index will indicate the richness of the habitat, in other words, this type of habitat has a large population and due to competition between species, will try to leave it. The opposite is true of habitats that are less populated and more likely to migrate. Two common interpretations of the verb Migration will be considered. The first view of habitat migration or Immigration, which determines the migration of the habitat, and its normalized numerical value is expressed by the lamp factor λ. The next view of migration from habitat or Emigration, which indicates the intensity of migration and in which the normalized numerical value is expressed with a nou coefficient μ. The location of habitats, such as decision variables in the response space, is denoted by the SIV symbol. In the migration process, this is done from habitats that are more populated and have a high migration coefficient μ to habitats with a high migration coefficient λ. In order to be located in different areas of the search space, the mutation stage of the variables takes place simultaneously with the migration stage. The basic steps of the algorithm in standard mode are discussed below.

4.2.1 Basic steps in biogeography-based optimization

Step 1. Production of a set of primary geographical habitats: In this initial step, we randomly form the *npop* number of habitats within the decision space of the variables. Then we evaluate and sort the objective function for the initial habitats.

Step 2. Calculate the numerical values of the normalization factors of immigration λ and emigration μ for each habitat.

Step 3. For each selected habitat such as i, repeat steps 4 to 6 to the initial population.

Step 4. For each variable such as k in location i, we repeat steps 5 to 6 to the number of array variables.

Step 5. With the probability λ_i for the variable x_{ik} and the origin of migration x_{jk} with the immigration coefficient μ, the location of the new habitat is determined according to the Eqs. (23) and (24):

$$if\ \mathbf{rand} \le lambda(i) \ \Rightarrow\ x_i^{new} = x_{ik} + \alpha_k \times (x_{jk} - x_{ik}), \quad (23)$$

$$\alpha_k = 0.9 . \quad (24)$$

In the original version, an alpha value of 0.9 was suggested.

Step 6. With the possibility of *pmutation*, on the selected variable x_{ir}, the mutation changes are performed according to the following conditions and with a specific random distribution (preferably normal distribution). The habitat position is determined after applying the mutation according to Eqs. (25) and (26):

$$if\ \mathbf{rand} \le pmutation \ \Rightarrow\ x_{ik}^{mut} = x_{ik}^{new} + sigma \times randn, \quad (25)$$

$$sigma = 0.02 \times (VarMax - VarMin). \quad (26)$$

In this regard, *Sigma* comprises a percentage of the decision space. In the original version, this value is 2%.

Step 7. Migration responses, mutations and previous responses are combined and after evaluation and sorting, up to *npop* are selected from the best of them as the next stage habitats.

Step 8. Termination conditions are checked and if necessary, the operation is repeated from step 3.

4.2.2 Chaos enhanced biogeography-based optimization (CBBO)

In the recent algorithm, to access the new habitat location, two migration and mutation strategies are performed, which correspond to exploitation and exploration, respectively. During the migration phase from x_{jk} to x_{ik}, local surveys are carried out in the neighborhood of the habitats and the optimal responses related to that area are determined. Also, by applying the mutation solution, the algorithm gets out of the trap of local optimization and leads to global optimization. As a result, the mutation phase saves the algorithm from the risk of premature convergence. If the random distributions of these two steps are replaced with chaos maps, it will significantly improve the performance of the algorithm. The proposed scenarios for this replacement are as follows:

Scenario 1. Placement of the chaos map in the migration stage of variables: In this case, the first **CHM1** chaos map in Eq. (23) replaces random selection and the result will be Eq. (27):

$$if\ \mathbf{CHM1} \le lambda(i) \ \Rightarrow\ x_{ik}^{new} = x_{ik} + \alpha_k \times (x_{jk} - x_{ik}). \quad (27)$$

Scenario 2. Placement of the chaos map in the stage of mutational changes of variables: In this case, the second **CHM2** chaos map in Eq. (25) replaces random selection and the result will be Eq. (28):

$$if\ \mathbf{CHM2} \le pmutation \ \Rightarrow\ x_{ik}^{mut} = x_{ik}^{new} + sigma \times randn. \quad (28)$$

Scenario 3. Placing the chaos map in both stages simultaneously: In this case, the two chaos maps are replaced simultaneously in Eqs. (23) and (25).

4.3 Standard teaching-learning-based optimization (TLBO)

This algorithm was proposed by Rao et al. [30] in 2011. The source of inspiration for this algorithm is the classroom learning process and, like many algorithms, it is population-based. In this algorithm, first an initial population of students is formed. This selection is random and is done within the search space. Then, two basic phases will be followed to correct the initial answers. The first phase is known as the teacher phase and is suggested to students based on the process of transferring knowledge from the teacher to the students. In this phase, the average academic level of the class is improved by the knowledge transferred through the teacher. It should also be noted that in this algorithm, there is practically no teacher and the best student in each course is recognized as a teacher. The second phase is known as the student phase, in which students learn about each other and their interactions with each other.

4.3.1 Basic steps in Standard teaching-learning-based optimization

Step 1. Formatting the basic parameters of the algorithm. These parameters include the student population *nL*,

the number of decision variables *nV*, the maximum number of repetitions of NFEs, which is also known as the stop criterion.

Step 2. Form the initial student population and evaluate it: Given the limitation of the search space, this population is formed randomly. Then, by applying the objective function, the answers are evaluated and sorted them.

Step 3. Out of the sorted population, the best of them are selected as *T* teachers. Then, the average position of the students is calculated and based on the teacher phase, the students' improved academic level is determined based on the Eqs. (29) and (30):

$$stepsizeT_i = T - TF_i \times MeanL\,, \tag{29}$$

$$\begin{aligned} &newL = L + \mathbf{rand}_{\mathbf{i,j}} \times stepsizeT \\ &i = 1,2,...,nL \;\; and \;\; j = 1,2,...,nV. \end{aligned} \tag{30}$$

In these relationships, the *TF* is teaching factor that randomly selected as 1 or 2, and indicates the teacher's success in increasing the average level of students. Finally, if the values of the evaluation are better than the previous values, the results replace them.

Step 4. In the student phase, the interactions of the students with each other are examined. In this phase, each student exchanges information with another randomly selected student (except himself/herself). The possibility of improving information is possible when the performance of the selected student is better, in which case their position changes according the Eqs. (31) and (32):

$$\begin{cases} if \;\; PFIT_i < PFIT_{rp} \;\; \Rightarrow \;\; stepsizeS_i = L_i - Lrp \\ f \;\; PFIT_i > PFIT_{rp} \;\; \Rightarrow \;\; stepsizeS_i = Lrp - L_i \end{cases}, \tag{31}$$

$$\begin{aligned} &newL = L + \mathbf{rand}_{\mathbf{i,j}} \times stepsizeS \\ &i = 1,2,...,nL \;\; and \;\; j = 1,2,...,nV \end{aligned} \tag{32}$$

The values obtained are evaluated and if they are better than the previous values, they are replaced. The best of the populations are introduced at each stage.

Step 5. Termination conditions are checked and if necessary, the operation is repeated from step 2.

4.3.2 Chaos enhanced teaching-learning-based optimization (CTLBO)

The process of teaching and learning in the classroom is the inspiration for this algorithm Which is mainly examined in two phases. These phases include the teacher's effect on the learning process and the students' interaction with each other, which play a significant role in the exploration and exploitation process, respectively. In each of these phases, random selections can be replaced by series of chaos maps. These maps are suggested to improve the exploration, exploitation, or both steps simultaneously. Therefore, the proposed scenarios for this replacement are as follows:

Scenario 1. Replacement of the chaos map in the teacher effect phase in the learning process: In this case, the first chaos function **CHM1** is replaced in Eq. (30) and the result will be Eq. (33):

$$newL = L + \mathbf{CHM1}_{\mathbf{i,j}} \times stepsizeT\,. \tag{33}$$

Scenario 2. Replacing the chaos map in the students' interaction phase with each other: In this case, the second of the **CHM 2** map function is replaced in Eq. (32) and the result will be Eq. (34):

$$newL = L + \mathbf{CHM2}_{\mathbf{i,j}} \times stepsizeS\,. \tag{34}$$

Scenario 3. Placing the chaos function in both steps simultaneously: In this case, the two chaos maps are replaced simultaneously in Eqs. (30) and (32).

4.4 Standard particle swarm optimization (PSO)

This algorithm is the most famous and most widely used meta-heuristic algorithm after the genetic algorithm. The domain is influenced by the algorithm with continuous variables and its idea was introduced by Kennedy and Eberhart [7]. In this algorithm, a number of particles are scattered in the search space, which is evaluated by applying each particle in the objective function, its criteria and value. By combining the previous velocity, the best position for each period of populations, and the best position for all population periods, the new position of each particle can be determined. In this case, to move from the existing position to the new position, the velocity vector is formed and added to the existing position. The components that participate in the velocity vector are: the coefficient of the previous velocity, the coefficient of the best local position of the course, and the coefficient of the best position of the whole best global position of the course. The vector composition of these components is shown in Fig. 3.

4.4.1 Basic steps in particle swarm optimization

Step 1. Random formation of the initial population of particles and evaluation of each of them.

Step 2. Determine the best particle for each population period and the best particle for the global population period.

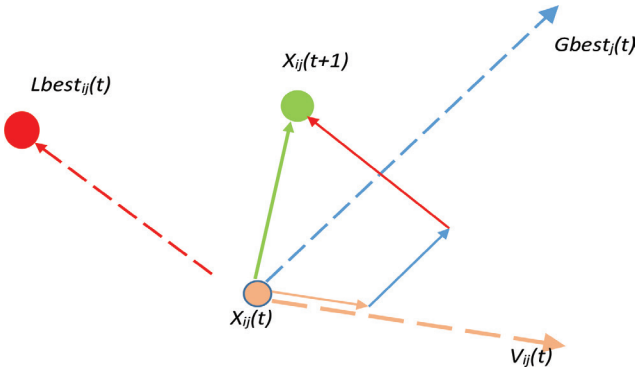

Fig. 3 Method to determine the new position in the particle for PSO

Step 3. Update the velocity vector and position vector based on the Eqs. (35) and (36).

$$\begin{aligned} v_{ij}(t+1) &= W \times v_{ij}(t) \\ &+ C_1 \times \mathbf{rand_{1j}(t)} \times \left\{ Lbest_{ij}(t) - X_{ij}(t) \right\} \\ &+ C_2 \times \mathbf{rand_{2j}(t)} \times \left\{ Gbest_j(t) - X_{ij}(t) \right\} \end{aligned} \tag{35}$$

$$X_{ij}(t+1) = X_{ij}(t) + v_{ij}(t+1) \tag{36}$$

In these relations W, the coefficient of inertia is usually chosen in the range of 0.4 to 0.9. C_1 and C_2 are also personal and collective learning coefficients, respectively. In the original version, the algorithm is proposed for both coefficients of zero to two.

Step 4. Check the termination conditions and repeat the operation from step 2 if necessary.

4.4.2 Chaos enhanced particle swarm optimization (CPSO)

This algorithm consists of two important positions, including the best position of each period and the best position of all periods, and to increase the variety in the search space, each is accompanied by a random coefficient. By replacing the chaos functions in the random selection of each of the periods, we will see a significant improvement in the performance of the algorithm. The proposed scenarios for this replacement are as follows:

Scenario 1. Insert the chaos function as the coefficient of the best position of each period: In this case, the first chaos function **CHM1** in Eq. (35) replaces the random distribution that the result will be Eq. (37).

$$\begin{aligned} v_{ij}(t+1) &= W \times v_{ij}(t) \\ &+ C_1 \times \mathbf{CHM_{1j}(t)} \times \left\{ Lbest_{ij}(t) - X_{ij}(t) \right\} \\ &+ C_2 \times \mathbf{rand_{2j}(t)} \times \left\{ Gbest_j(t) - X_{ij}(t) \right\} \end{aligned} \tag{37}$$

Scenario 2. Positioning the chaos function as the coefficient of the best position of all periods: In this case, the second chaos function **CHM2** in Eq. (35) replaces the random distribution and the result will be Eq. (38).

$$\begin{aligned} v_{ij}(t+1) &= W \times v_{ij}(t) \\ &+ C_1 \times \mathbf{rand_{1j}(t)} \times \left\{ Lbest_{ij}(t) - X_{ij}(t) \right\} \\ &+ C_2 \times \mathbf{CHM_{2j}(t)} \times \left\{ Gbest_j(t) - X_{ij}(t) \right\} \end{aligned} \tag{38}$$

Scenario 3. Placing both turbulence functions as coefficients of the best position of each period and all periods: In this case, both chaos maps simultaneously replace the random distribution in Eq. (35).

5 Numerical examples of optimal truss design

In this research, to compare the efficiency of algorithms in standard and chaotic mode, several optimization examples from the truss group have been selected. The purpose of the optimal design of truss structures is to select the lowest possible value for the cross-sectional area of the members, which at the same time satisfies the limitations related to the vibration frequency in different modes to avoid the destructive phenomenon of resonance and shake. The standard mode of each algorithm is examined along with 9 different turbulence modes. In this challenging competition, the final optimal mode is selected from forty optimization designs with different methods and inspirations. Given the vast statistical space for optimal design, we will have intense challenge and competition for the desire for absolute optimality. Therefore, the possibility of accessing optimal global responses with high accuracy has increased. Other important results in this research can be access to the best algorithm, the best chaos function and the best scenario.

5.1 A 52-bar dome-like truss

The 52-bar dome-like truss as shown in Fig. 4 is a well-known benchmark problem for optimizing the weight and shape of trusses with frequency constraints. This truss considers both optimizations of the section size and geometric coordinates of the nodes and the geometric shape of the structure is determined during the optimization process. The decision variables related to the section size are classified into 8 groups according to the symmetry in the geometric shape. Geometric coordinates of all symmetric free nodes can be changed by 2 m from the initial position along the coordinate axes. In this case, the number of decision variables related to the shape of the

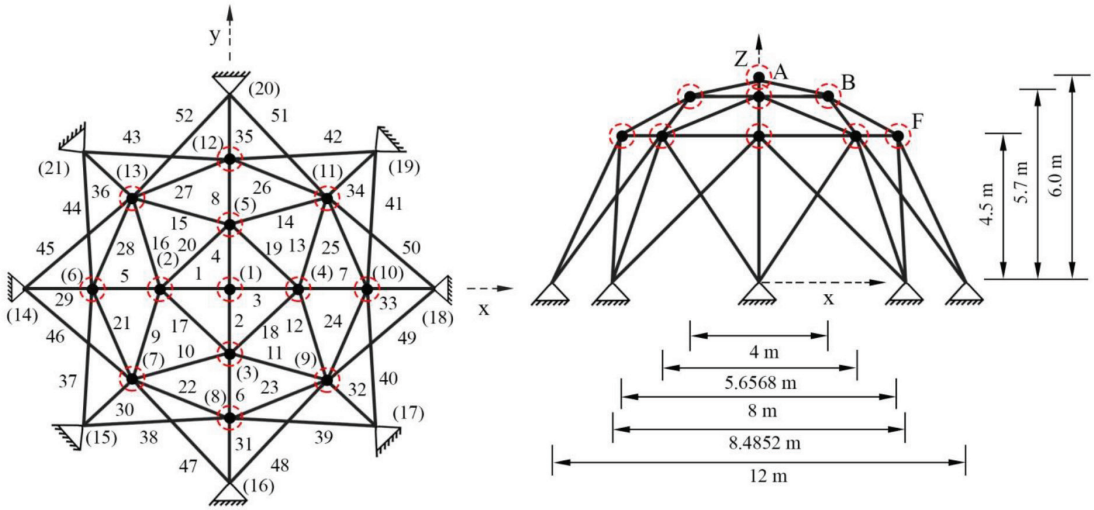

Fig. 4 Schematic of the 52-bar dome-like truss

structure and the geometric coordinates of the nodes is limited to 5 variables, and the sum of the variables, including shape and size, will be 13 variables. In all free nodes, a non-structural concentrated mass of 50 kg has affected all free nodes. The mechanical characteristics of the structure are: density of materials 7800 kg/m^3, modulus of elasticity 210000 MPa, frequency limitations of the structure in the first mode are less than 15.916 Hz and in the second mode are greater than 28.648 Hz. For the cross section of the members, the lower limit is 1 cm^2 and the upper limit is 10 cm^2.

In order to ensure the performance of turbulent functions and algorithms, as well as to increase the accuracy and sensitivity of calculations, each of the modes has been performed independently 20 times and the results related to the best response and the average value of responses are presented in Statistical Table 1. Also, the coefficient of variation of responses, which is a measure of the robustness and robustness of responses, has been calculated and used to compare the efficiency of turbulence functions and algorithms. For quick access to optimization information, a bar chart of each component is shown in Fig. 5.

Table 1 Statistical results for the 52-bar dome-like truss

Algorithms	Best	Mean	C.V(%)	Algorithms	Best	Mean	C.V(%)
CPA	193.923	195.7598	1.8703	BBO	195.8181	208.6882	5.0975
Gauss-1 → CCPA-21	**193.0961**	195.4159	1.8663	Gauss-1 → CBBO-21	193.8629	196.0034	1.1143
Gauss-2 → CCPA-22	193.3469	197.2374	2.3584	Gauss-2 → CBBO-22	194.1574	201.1911	3.8191
Gauss-3 → CCPA-23	193.7925	200.5983	2.8589	Gauss-3 → CBBO-23	192.7193	196.6800	2.0702
Liebovitch-1 → CCPA-31	193.2595	197.0165	2.4719	Liebovitch-1 → CBBO-31	192.5337	197.4691	1.7329
Liebovitch-2 → CCPA-32	193.1753	194.9615	1.9749	Liebovitch-2 → CBBO-32	192.7333	197.6173	2.1936
Liebovitch-3 → CCPA-33	193.1893	**193.3202**	**0.070826**	Liebovitch-3 → CBBO-33	193.2867	193.6394	**0.1599**
Piecewise-1 → CCPA-41	193.2122	195.3727	2.0864	Piecewise-1 → CBBO-41	**192.0430**	196.4254	1.3519
Piecewise-2 → CCPA-42	193.5432	198.5575	3.3370	Piecewise-2 → CBBO-42	192.2379	194.5195	1.6893
Piecewise-3 → CCPA-43	193.3756	199.4612	2.8877	Piecewise-3 → CBBO-43	192.9604	**193.6064**	0.27667
TLBO	194.7714	199.4808	1.7479	PSO	193.9358	201.3898	3.4257
Gauss-1 → CTLBO-21	192.9113	196.5568	2.4440	Gauss-1 → CPSO-21	192.2222	194.9346	2.0445
Gauss-2 → CTLBO-22	192.921	193.0511	**0.04594**	Gauss-2 → CPSO-22	192.0872	195.1317	1.9772
Gauss-3 → CTLBO-23	192.9099	193.0708	0.048783	Gauss-3 → CPSO-23	193.2182	195.3024	1.8885
Liebovitch-1 → CTLBO-31	192.9511	194.8092	2.0155	Liebovitch-1 → CPSO-31	193.1628	195.0924	1.8887
Liebovitch-2 → CTLBO-32	**192.5833**	**193.0411**	0.1338	Liebovitch-2 → CPSO-32	193.1340	198.3994	2.2896
Liebovitch-3 → CTLBO-33	193.0481	194.8546	2.0017	Liebovitch-3 → CPSO-33	**192.0444**	197.7078	2.5092
Piecewise-1 → CTLBO-41	193.0055	198.3462	2.4248	Piecewise-1 → CPSO-41	193.2837	**193.4978**	**0.089781**
Piecewise-2 → CTLBO-42	192.8472	196.9014	2.3152	Piecewise-2 → CPSO-42	193.3386	198.4962	2.3546
Piecewise-3 → CTLBO-43	192.9188	193.1454	0.068056	Piecewise-3 → CPSO-43	192.5061	197.7143	2.2578

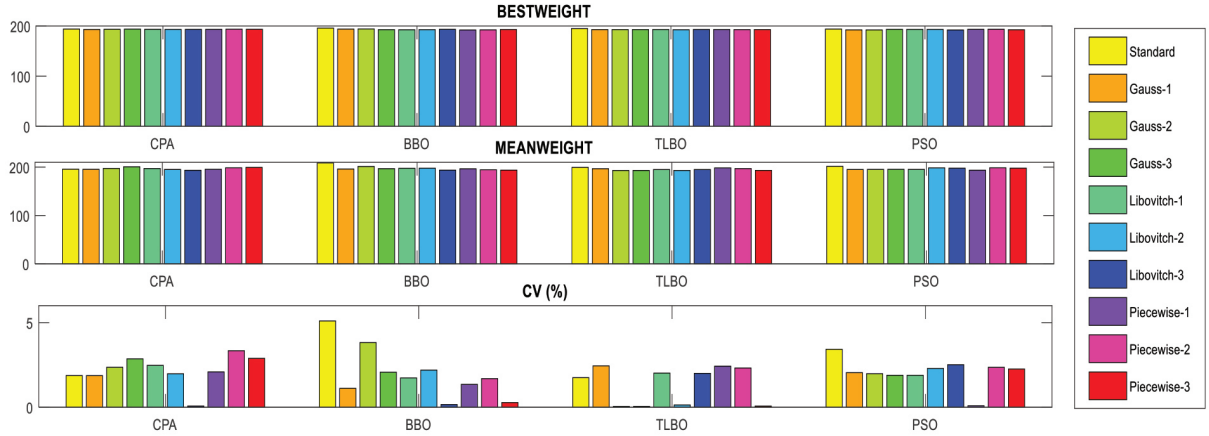

Fig. 5 Optimization results in standard mode and selection of chaos map for the 52-bar dome-like truss

Examining the optimization results for different combinations of algorithms with turbulence functions and comparing it with the standard mode, shows a significant and significant improvement in reducing the weight of the 52-bar dome-like truss. The results for each of the algorithms are:

In the cyclic parthenogenesis algorithm, the Gaussian chaos map with Scenario 1 with a weight of 193.0961 kg has the optimal response. In the biogeography-based optimization, the piecewise chaos map with Scenario 1 with a weight of 192.0430 kg has the optimal response. In the teaching-learning-based optimization, the Liebovitch chaos map with Scenario 2 with a weight of 192.5833 kg has the optimal answer, and finally, in the particle swarm optimization, the Liebovitch chaos map with Scenario 3 weighs 192.0444 kg has the optimal answer. Also, in Table 2, the results of this research are compared with a number of previous research [37–41].

Table 2 Optimal design comparison for the 52-bar dome-like truss

Decision Variable	Lingyun et al. [37]	Gomes [38]	Liu et al. [39]	Kaveh et al. [40]	Kaveh et al. [41]	CCPA-21 Present Work	CBBO-41 Present Work	CTLBO-32 Present Work	CPSO-33 Present Work
Z_A (m)	5.8851	5.5344	4.3201	6.5299	5.9362	5.9182	4.5375	6.0600	5.7898
X_B (m)	1.7623	2.0885	1.3153	2.2898	2.2416	2.2612	1.8920	2.3427	2.0450
Z_B (m)	4.4091	3.9283	4.1740	4.0066	3.7309	3.7000	4.2890	3.7563	3.7510
X_F (m)	3.4406	4.0255	2.9169	4.1712	3.9630	3.9427	3.8453	4.0319	3.8833
Z_F (m)	3.1874	2.4575	3.2676	2.5000	2.5000	2.5000	2.7713	2.5002	2.5039
A_1 (cm^2)	1.0000	0.3696	1.0000	1.0000	1.0001	1.0000	1.0002	1.0003	1.0032
A_2 (cm^2)	2.1417	4.1912	1.3300	1.1099	1.1654	1.1162	1.0028	1.0275	1.2823
A_3 (cm^2)	1.4858	1.5123	1.5800	1.1806	1.2323	1.2153	1.4596	1.1561	1.2531
A_4 (cm^2)	1.4018	1.5620	1.0000	1.2305	1.4323	1.4581	1.3772	1.4522	1.5536
A_5 (cm^2)	1.9110	1.9154	1.7100	1.5532	1.3901	1.3884	1.3009	1.4181	1.3918
A_6 (cm^2)	1.0109	1.1315	1.5400	1.0051	1.0001	1.0000	1.0000	1.0000	1.0087
A_7 (cm^2)	1.4693	1.8233	2.6500	1.4133	1.6024	1.6456	1.3272	1.5555	1.4733
A_8 (cm^2)	2.1411	1.0904	2.8700	1.5415	1.4131	1.3351	1.5643	1.3914	1.4285
Best Weight(kg)	236.046	228.381	298.0	197.462	194.85	193.0961	192.0430	192.5833	192.0444
Mean Weight(kg)	N/A	N/A	N/A	199.72	196.85	195.4159	196.4254	193.0411	197.7078
Coefficient Variation (CV)	N/A	N/A	N/A	1.6323	1.2090	1.8663	1.3519	0.1338	2.5092
NFE	N/A	N/A	N/A	6000	N/A	25000	40850	30350	24040
ω_1 (HZ)	12.81	12.751	15.22	11.421	11.4339	11.4909	15.8567	11.7997	10.5713
ω_2 (HZ)	28.65	28.649	28.649	29.28	28.6480	28.6391	28.6523	28.6888	28.6785

5.2 A 120-bar spatial dome

The 120-bar spatial dome as shown in Fig. 6 is a well-known benchmark problem with weight-limit optimization. This truss only considers optimizing the size of the sections and the geometric shape of the structure is constant during the optimization process. The decision variables related to the size of the members' sections and according to the symmetry in the geometric shape of the dome along the X and Y axes, are classified into 7 groups. Non-structural concentrated mass in all free nodes affects the structure. Their values are 3 kg in node 1, 500 kg in nodes 2 to 13 and 100 kg in other nodes. The mechanical characteristics of the structure are: material density 7971.81 kg/m^3, modulus of elasticity 210,000 MPa, frequency limits of the structure in the first and second modes are greater than 9 and 11 Hz, respectively. For the cross section of the members, the range of the lower limit is 1 cm^2 and the upper limit is 129.3 cm^2. In order to ensure the performance of chaos map and algorithms, as well as to increase the accuracy and sensitivity of calculations, each of the modes has been performed independently 20 times and the results related to the best response and the average value of responses are presented in Statistical Table 3. Also, the coefficient of change of responses, which is a measure of the robustness and robustness of responses, has been calculated and used to compare the efficiency of turbulence functions and algorithms. For quick access to optimization information, the bar chart of each component is shown in Fig. 7.

Examining the optimization results for different combinations of algorithms with turbulence functions and comparing it with the standard mode, shows a significant and significant improvement in reducing the weight of the 120-bar spatial dome. The results for each of the algorithms are:

In the cyclic parthenogenesis algorithm, the Liebovitch chaos map with Scenario 3 with a weight of 8709.3186 kg has the optimal response. In the biogeography-based optimization, the Gaussian chaos map with Scenario 3 with a weight of 1064.8710 kg has the optimal response. In the teaching-learning-based optimization, the Liebovitch chaos map with Scenario 3 with a weight of 5095.8708 kg has the optimal answer, and finally, in the particle swarm optimization, the Liebovitch chaos map with Scenario 1 weighs 8709.1357 kg of the optimal response. Also, in Table 4, the results of this research are compared with a number of previous research [41–43].

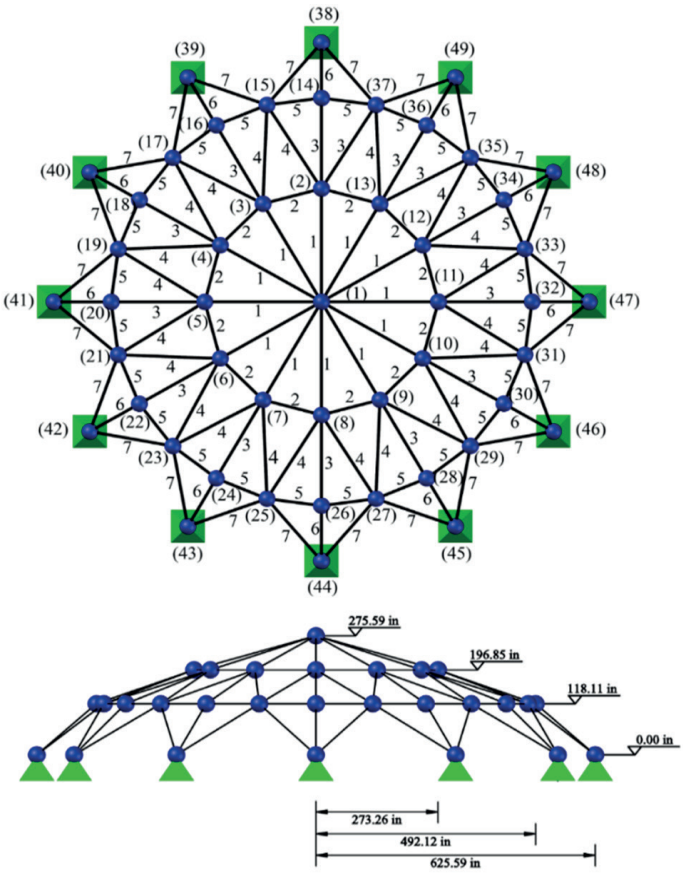

Fig. 6 Schematic of the 120-bar spatial dome

Table 3 Statistical results for the 120-bar spatial dome

Algorithms	Best	Mean	C.V(%)	Algorithms	Best	Mean	C.V(%)
CPA	8714.4176	8727.3576	0.12780	BBO	8724.4232	8758.7686	0.33832
Gauss-1 → CCPA-21	8711.1341	8714.6874	0.047296	Gauss-1 → CBBO-21	8713.8710	8767.8780	0.74910
Gauss-2 → CCPA-22	8710.8383	8720.2623	0.070094	Gauss-2 → CBBO-22	8715.0951	8739.4275	0.42259
Gauss-3 → CCPA-23	8710.0810	8715.9243	0.068405	Gauss-3 → CBBO-23	**8710.1064**	8732.1659	0.36668
Liebovitch-1 → CCPA-31	8709.9563	8715.4375	0.040882	Liebovitch-1 → CBBO-31	8718.2432	8732.2834	0.15313
Liebovitch-2 → CCPA-32	8709.9641	8712.0198	0.020616	Liebovitch-2 → CBBO-32	8718.4498	8736.9097	0.18282
Liebovitch-3 → CCPA-33	**8709.3186**	**8711.4911**	**0.015666**	Liebovitch-3 → CBBO-33	8712.0282	8740.0212	0.30298
Piecewise-1 → CCPA-41	8709.6518	8717.7547	0.091054	Piecewise-1 → CBBO-41	8712.4152	8727.5799	0.15603
Piecewise-2 → CCPA-42	8712.8968	8718.9102	0.068468	Piecewise-2 → CBBO-42	8718.4704	8735.2244	0.16733
Piecewise-3 → CCPA-43	8711.5232	8715.7299	0.042128	Piecewise-3 → CBBO-43	8712.9988	**8719.4447**	**0.071687**
TLBO	8713.1479	8716.1568	0.026596	PSO	8713.1316	8721.2938	0.10558
Gauss-1 → CTLBO-21	8708.6610	8709.5695	0.010765	Gauss-1 → CPSO-21	8709.1708	8715.6655	0.052448
Gauss-2 → CTLBO-22	8708.6101	8709.6159	0.009924	Gauss-2 → CPSO-22	8710.1033	8714.1660	**0.031257**
Gauss-3 → CTLBO-23	8708.8308	8709.8127	0.015615	Gauss-3 → CPSO-23	8709.7487	8716.7589	0.071588
Liebovitch-1 → CTLBO-31	8708.6722	**8708.9507**	**0.0019348**	Liebovitch-1 → CPSO-31	**8709.1357**	8713.9009	0.046184
Liebovitch-2 → CTLBO-32	8708.7561	8709.6450	0.013158	Liebovitch-2 → CPSO-32	8710.8816	**8713.7953**	0.03573
Liebovitch-3 → CTLBO-33	**8708.5095**	8709.3689	0.009658	Liebovitch-3 → CPSO-33	8714.3378	8721.3876	0.086145
Piecewise-1 → CTLBO-41	8708.8503	8709.2576	0.0054369	Piecewise-1 → CPSO-41	8712.9719	8717.5149	0.042645
Piecewise-2 → CTLBO-42	8708.6157	8709.2453	0.0056748	Piecewise-2 → CPSO-42	8709.6996	8719.5143	0.10432
Piecewise-3 → CTLBO-43	8709.1047	8709.8531	0.0077434	Piecewise-3 → CPSO-43	8709.8949	8718.6591	0.096190

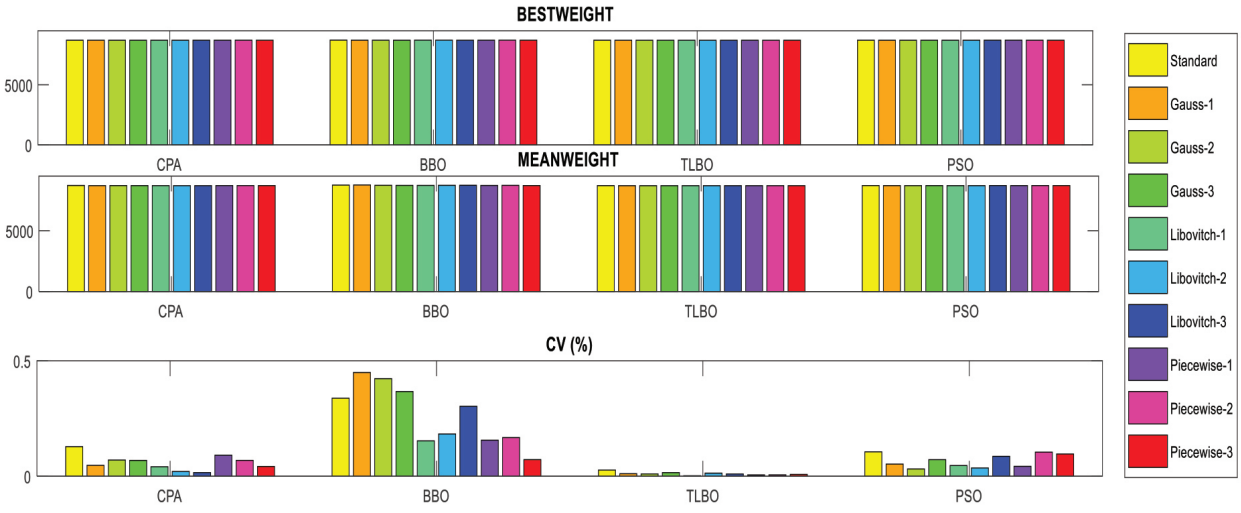

Fig. 7 Optimization results in standard mode and selection of the chaos map for the 120-bar spatial dome

5.3 A 200-bar planar truss structure

The 200-bar planar truss structure as shown in Fig. 8 is a well-known benchmark problem for weight optimization with frequency limits. This truss only considers optimizing the size of the sections and the geometric shape of the structure is constant during the optimization process. The decision variables related to the sections size of the members are classified into 29 groups. Non-structural concentrated mass in nodes 1 to 5 and in the amount of 100 kg affect the structure. The mechanical characteristics of the structure are: material density 7860 kg/m^3, modulus of elasticity 210,000 MPa, frequency limits of the structure in the first, second and third modes are greater than 5, 10 and 15 Hz, respectively. For the cross section of the members, the lower limit range is 0.1 cm^2 and the upper limit is 25 cm^2. In order to ensure the performance of turbulent functions and algorithms, as well as to increase the accuracy and sensitivity of calculations, each of the modes has been

Table 4 Optimal design comparison for the 120-bar spatial dome

Decision Variable	Kaveh and Zolghadr [8]	Kaveh and Ilchi Ghazaan [22]	Kaveh and Ilchi Ghazaan [41]	Tejani et al. [42]	Khatibinia and Naseralavi [43]	CCPA-33 Present Work	CBBO-23 Present Work	CTLBO-33 Present Work	CPSO-31 Present Work
A_1	19.607	19.6836	19.8905	19.5203	20.263	19.6393	19.4744	19.5140	19.6213
A_2	41.290	40.9581	40.4045	40.8482	39.294	40.2495	40.0237	40.3250	39.9903
A_3	11.136	11.3325	11.2057	10.3225	9.989	10.6283	10.7416	10.6250	10.7143
A_4	21.025	21.5387	21.3768	20.9277	20.563	21.1317	21.1947	21.0889	21.2248
A_5	10.060	9.8867	9.8669	9.6554	9.603	9.64102	10.1090	9.8693	9.7974
A_6	12.758	12.7116	12.7200	12.1127	11.738	11.7325	11.7152	11.7806	11.6808
A_7	15.414	14.9330	15.2236	15.0313	15.877	14.9045	14.7183	14.8565	14.7918
Best Weight (kg)	8890.48	8888.74	8889.96	8713.3030	8724.97	8709.3186	8710.1064	8708.5095	8709.1357
Mean Weight (kg)	N/A	8896.04	8900.39	8735.3452	8745.58	8711.4911	8732.1659	8709.3689	8713.9009
Coefficient Variation (CV)	N/A	0.07475	0.0716	0.2049	0.0135	0.015666	0.36668	0.009658	0.046184
NFE	N/A	30000	17000	4000	242700	30000	53000	30350	32040
ω_1 (HZ)	9.0001	9.000	9.000	9.0009	9.002	9.000	9.000	9.000	9.000
ω_2 (HZ)	11.0007	11.000	11.000	11.0005	11.003	11.000	11.000	11.000	11.000

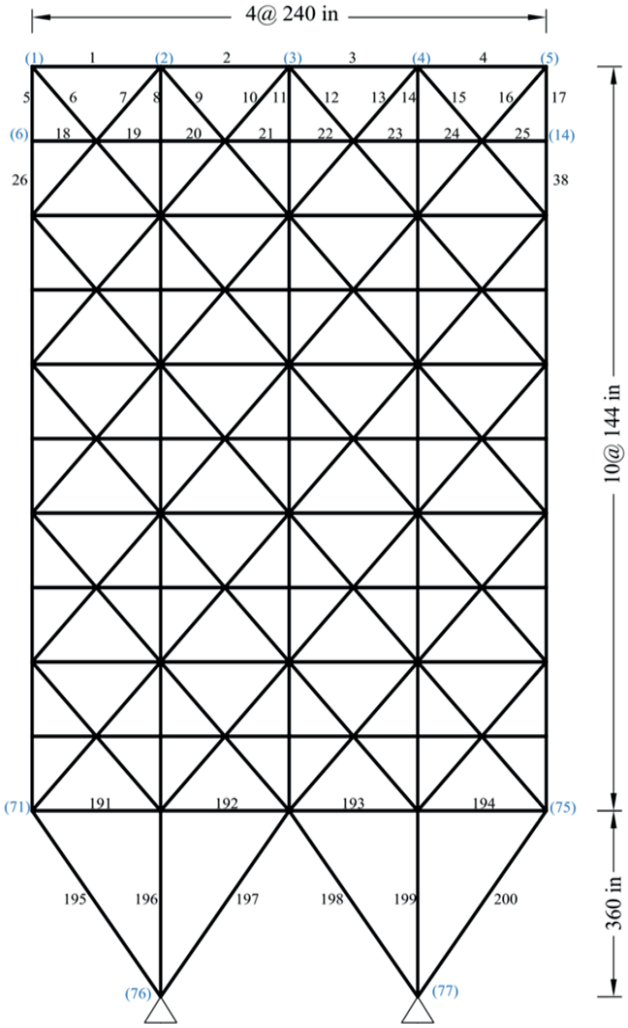

Fig. 8 Schematic of a 200-bar planar truss structure

performed independently 20 times and the results related to the best response and the average value of responses are presented in Statistical Table 5. Also, the coefficient of change of responses, which is a measure of the robustness and robustness of responses, has been calculated and used to compare the efficiency of turbulence functions and algorithms. For quick access to optimization information, a bar chart of each component is shown in Fig. 9.

Examining the optimization results for different combinations of algorithms with turbulence functions and comparing it with the standard mode, shows a significant and significant improvement in reducing the weight of the 200-bar planar truss structure. The results for each of the algorithms are:

In the cyclic parthenogenesis algorithm, the Liebovitch chaos map with Scenario 2 with a weight of 2157.2685 kg has the optimal response. In the biogeography-based optimi-

Table 5 Statistical results for the 200- bar planar truss structure

Algorithms	Best	Mean	C.V(%)	Algorithms	Best	Mean	C.V(%)
CPA	2163.2600	2170.2616	0.25081	BBO	2183.9321	2192.0868	0.46106
Gauss-1 → CCPA-21	2157.7905	2160.8575	0.23417	Gauss-1 → CBBO-21	2163.5970	**2165.6248**	**0.093395**
Gauss-2 → CCPA-22	2158.2989	2160.1782	0.085413	Gauss-2 → CBBO-22	2164.1197	2173.6170	0.29618
Gauss-3 → CCPA-23	2157.6699	2159.2446	0.10542	Gauss-3 → CBBO-23	2162.2921	2172.4986	0.36184
Liebovitch-1 → CCPA-31	2158.0615	2159.7250	0.084546	Liebovitch-1 → CBBO-31	2161.6518	2169.2719	0.22424
Liebovitch-2 → CCPA-32	**2157.2685**	2159.2455	0.14705	Liebovitch-2 → CBBO-32	**2161.5657**	2168.7783	0.20266
Liebovitch-3 → CCPA-33	2157.6223	2158.8040	**0.049231**	Liebovitch-3 → CBBO-33	2165.2998	2169.9402	0.26866
Piecewise-1 → CCPA-41	2157.4065	**2158.7347**	0.052349	Piecewise-1 → CBBO-41	2163.3718	2167.1790	0.12069
Piecewise-2 → CCPA-42	2158.5338	2164.5214	0.37636	Piecewise-2 → CBBO-42	2165.0191	2170.9598	0.41980
Piecewise-3 → CCPA-43	2158.6010	2162.9471	0.30742	Piecewise-3 → CBBO-43	2165.6825	2175.7005	0.31631
TLBO	2160.9171	2164.2801	0.15306	PSO	2170.8269	2173.7456	0.14449
Gauss-1 → CTLBO-21	2157.9566	2159.2716	**0.058363**	Gauss-1 → CPSO-21	2158.0777	2158.9851	0.055937
Gauss-2 → CTLBO-22	2157.8314	2161.0117	0.16852	Gauss-2 → CPSO-22	2157.1382	2160.6052	0.12816
Gauss-3 → CTLBO-23	2157.9931	2161.0868	0.16428	Gauss-3 → CPSO-23	2157.0474	2158.2200	0.045259
Liebovitch-1 → CTLBO-31	2157.7175	2158.5939	0.063469	Liebovitch-1 → CPSO-31	2161.8257	2170.1612	0.32028
Liebovitch-2 → CTLBO-32	2157.8220	2158.6214	0.045414	Liebovitch-2 → CPSO-32	2168.9833	2183.6840	0.54788
Liebovitch-3 → CTLBO-33	2157.2139	2158.6594	0.050986	Liebovitch-3 → CPSO-33	2190.1487	2227.3864	2.0575
Piecewise-1 → CTLBO-41	**2156.8604**	2158.1933	0.089636	Piecewise-1 → CPSO-41	2157.1898	2157.8561	**0.025187**
Piecewise-2 → CTLBO-42	2157.0346	**2157.2344**	**0.0091923**	Piecewise-2 → CPSO-42	**2156.8582**	**2157.6555**	0.032237
Piecewise-3 → CTLBO-43	2157.1807	2157.7327	0.021611	Piecewise-3 → CPSO-43	2160.8278	2240.5533	4.8003

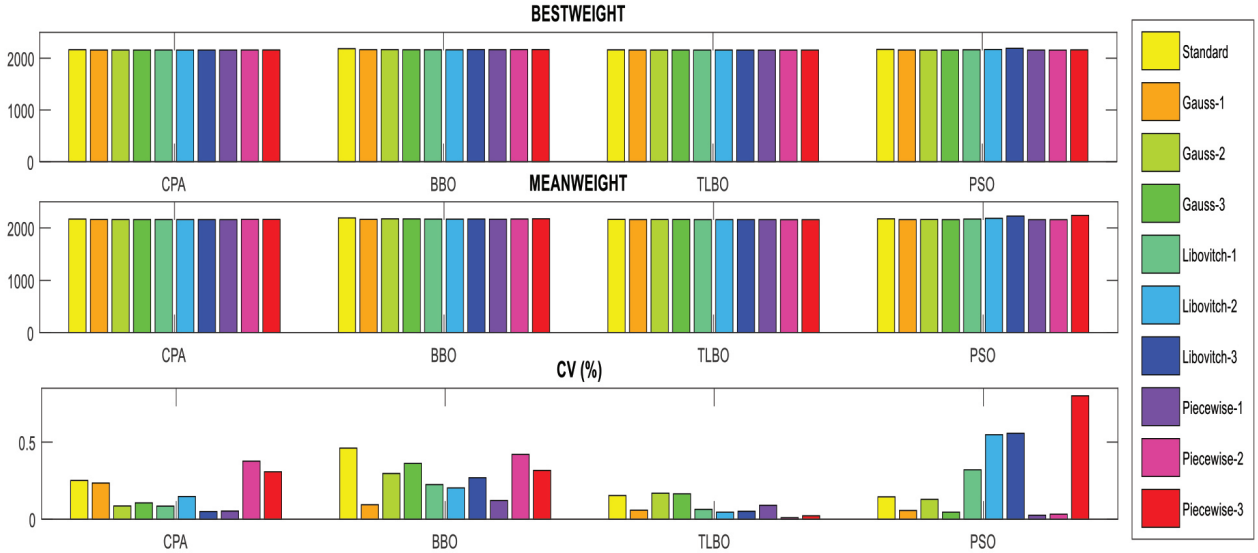

Fig. 9 Optimization results in standard and the chaos map for the 200- bar planar truss structure

zation, the Liebovitch chaos map with Scenario 2 with a weight of 215/5657 kg has the optimal answer. In the optimization algorithm based on teaching-learning-based optimization, the Piecewise chaos map with Scenario 1 with a weight of 2156/8604 kg has the optimal answer, and finally, in the particle swarm optimization, the Piecewise chaos map with Scenario 2 weighs 2156/8582 kg has an optimal response. Also, in Table 6 the results of this study are compared with a number of previous studies [41,44,45].

6 Discussions

In this paper, four meta- heuristic algorithms are investigated and made chaotic to increase the possibility of performing global optimization. Commonly in most of the meta-heuristic algorithms, an imbalance between the exploration and exploitation stages causes the algorithm to stop at local optimizations and premature convergence occurs for them. In a number of algorithms, the mutation stage scheme is attempted to be deployed in scattered areas of the search space and then the neighborhoods are examined. In most algorithms, the mutation cases of the algorithm alone are not effective and sufficient, and the chaos maps provide suitable conditions to accelerate the escape from the local optimal trap and by creating turbulence and disorder in the search space, the possibility of jumping to most scattered positions in the search space. It can be shown that the most important feature of chaos maps is to balance the exploration and exploitation stages. Research shows that chaos maps have good potential to provide this balance. By replacing these maps in the exploration, exploitation, or both, different scenarios for optimization are obtained. In this research, by applying chaos map in several groups of meta-heuristic algorithms, a significant improvement in the weight and shape optimization of trusses has been achieved. Also, in order to form a statistical population and determine the best weight, mean weight and coefficient of variation, each structural model has been implemented with 20 independent replications. To extract the final results, the processes related to the previous tables are combined and then normalized. The Eq. (39) is intended to combine and summarize the information of all the examples.

$$Val_{com}^{MV} = \frac{1}{S}\sum_{i=1}^{S}\left(\frac{Val^{MV}}{Val_{i,\min}} - 1\right) \tag{39}$$

Based on Eq. (39), the success rate of each of the 10 modes (standard mode with 9 turbulence modes) is determined separately for each algorithm. To determine them, the results of all examples are summarized and presented. In this relation, for each selected algorithm, Val^{Mv}, Val_{com}^{Mv} and $Val_{i,\min}$, respectively, the optimal values of the statistical tables for each example in each of the standard and chaotic modes, the minimum value among the 10 modes for the same example and the final result of the combination. The whole result is for the same state of the algorithm. Also, i and S are the number of optimized structural examples and the total number of examples, respectively. This relationship is formed for all three characteristics including optimal weight, optimal average and optimal coefficient of variation (CV). The criterion for choosing the best efficiency is related to the modes that have the lowest value. And in this regard, the results have not been normalized yet.

$$Val_{norm}^{MV} = \frac{\dfrac{1}{Val_{com}^{MV}}}{\sum_{j=1}^{nopt}\dfrac{1}{Val_{j,com}^{MV}}} \times 100 \tag{40}$$

Two things still need to be reviewed to make it easier to determine the optimal states. The first is to normalize the results and the second is to change the highest percentages to express the best performance. For this aim we can consider inverse functions. Both cases are considered in Eq. (40). In this regard, for each selected algorithm $Val^{MV}{}_{com}$, $Val^{MV}{}_{j,com}$, nopt and $Val^{MV}{}_{norm}$, respectively, the optimal values obtained for each of the 10 modes in the previous relation, the same values for summation, the total number of modes including standard and chaotic (This number is 10 here) and the optimal values are in percentage and normalized.

By applying Eqs. (39) and (40) to the total results of the optimizations performed, the final normalized results with the participation of all the examples are presented in Table 7.

Based on the final results, the optimal design for determining the best weight in the cyclical parthenogenesis algorithm belongs to the Liebovitch chaos map with the third scenario. the biogeography-based optimization belongs to the Piecewise chaos map with the first scenario. The teaching-learning-based optimization belongs to the Piecewise chaos map with the second scenario and the particle swarm optimization belong to the Gaussian chaos map with the second scenario. For swift access to optimal weight information, the pie charts of each of the chaos meta-heuristic algorithms are shown in Fig. 10.

Optimal design for determining the best mean in the cyclical parthenogenesis algorithm belonging to Liebovitch chaos map with third scenario, biogeography-based optimization belonging to piecewise chaos map with third scenario, the teaching-learning-based optimization belonging

Table 6 Optimal design comparison for the 200-bar planar truss structure

Number group	Element group	Kaveh and Kooshbaghi [41]	Kaveh and Ilchi Ghazaan [44] ALC-PSO	Kaveh and Zolghadr [45] CSS-BBBC	Kaveh and Zolghadr [45]	CCPA-32 Present Work	CBBO -32 Present Work	CTLBO -41 Present Work	CPSO -42 Present Work
1	1,2,3,4	0.3262	0.2750	0.2934	0.2439	0.2910	0.3270	0.2904	0.3021
2	5,8,11,14,17	0.4060	0.4264	0.5561	0.1438	0.4760	0.4687	0.4621	0.4543
3	19,20,21,22,23,24	0.1062	0.1000	0.2952	0.3769	0.1000	0.1000	0.1004	0.1000
4	18,25,56,63,94,101,132,139,170,177	0.1082	0.1000	0.1970	0.1494	0.1000	0.1000	0.1003	0.1000
5	26,29,32,35,38	0.4917	0.7000	0.8340	0.4835	0.5148	0.5241	0.5146	0.5040
6	6,7,9,10,12,13,15,16,27,28,30,31,33,34,36,37	0.8509	0.7948	0.6455	0.8103	0.8167	0.8717	0.8161	0.8218
7	39,40,41,42	0.1024	0.1003	0.1770	0.4364	0.1000	0.1044	0.1031	0.1003
8	43,46,49,52,55	1.4816	1.5402	1.4796	1.4554	1.4498	1.4867	1.4349	1.4248
9	57,58,59,60,61,62	0.1318	0.1000	0.4497	1.0103	0.1000	0.1000	0.1003	0.1002
10	64,67,70,73,76	1.6093	1.7544	1.4556	2.1382	1.5807	1.5346	1.6315	1.5866
11	44,45,47,48,50,51,53,54,65,66,68,69,71,72,74,75	1.1354	1.1213	1.2238	0.8583	1.1776	1.1560	1.1589	1.1471
12	77,78,79,80	0.1196	0.1000	0.2739	1.2718	0.1000	0.1519	0.1204	0.1257
13	81,84,87,90,93	3.0434	2.8381	1.9174	3.0807	3.0007	3.1039	2.9453	3.0128
14	95,96,97,98,99,100	0.3132	0.1000	0.1170	0.2677	0.1007	0.1137	0.1001	0.1024
15	102,105,108,111,114	3.2862	3.3936	3.5535	4.2403	3.3035	3.0955	3.2397	3.2897
16	82,83,85,86,88,89,91,92,103,104,106,107,109,110,112,113	1.5869	1.5849	1.3360	2.0098	1.5436	1.5843	1.5722	1.5804
17	115,116,117,118	0.2249	0.1000	0.6289	1.5956	0.2192	0.2098	0.2853	0.2150
18	119,122,125,128,131	5.0850	5.2642	4.8335	6.2338	5.1218	5.4634	5.0876	5.1509
19	133,134,135,136,137,138	0.1709	0.1000	0.6062	2.5793	0.1000	0.1000	0.1000	0.1000
20	140,143,146,149,152	5.2071	5.7884	5.4393	3.0520	5.6298	5.3221	5.4268	5.6133
21	120,121,123,124,126,127,129,130,141,142,144,145,147,148,150,151	2.2289	2.0218	1.8435	1.8121	2.1283	1.9342	2.0995	2.0780
22	153,154,155,156	0.2708	0.4600	0.8955	1.2986	0.5979	0.6489	0.7075	0.6979
23	157,160,163,166,169	8.0270	7.8414	8.1759	5.8810	7.6220	7.8271	7.6815	7.7415
24	171,172,173,174,175,176	0.2105	0.2983	0.3209	0.2324	0.1000	0.2432	0.1414	0.1223
25	178,181,184,187,190	7.8354	8.1844	10.9800	7.7536	8.0244	8.1843	7.8547	8.0971
26	158,159,161,162,164,165,167,168,179,180,182,183,185,186,188,189	2.9012	2.7756	2.9489	2.6871	2.7715	2.8095	2.8167	2.8186
27	191,192,193,194	9.5438	10.1639	10.5243	12.5094	w10.6055	10.8694	10.6712	10.5128
28	195,197,198,200	21.4380	21.4137	20.4271	29.5704	21.0961	20.7910	21.1478	21.0633
29	196,199	11.3070	10.9083	19.0983	8.2910	10.9458	11.3466	10.7367	10.7336
Best	Weight(kg)	2167.4954	2162.99	2298.61	2259.86	2157.268	2161.5657	2156.8604	2156.858
Mean	Weight(kg)	2180.3886	2562.07	N/A	N/A	2159.245	2168.7783	2158.1933	2157.655
	Coefficient Variation(CV)	0.3734	12.8236	N/A	N/A	0.14705	0.20266	0.089636	0.032237
NFE	N-function evaluation	23000	20000	N/A	10000	20000	35750	50550	36040
	ω_1 (HZ)	5.000	5.000	5.010	5.010	5.000	5.0002	5.000	5.000
	ω_2 (HZ)	12.3550	12.1360	12.911	12.911	12.0408	12.4891	12.1329	12.2060
	ω_3 (HZ)	15.0212	15.210	15.416	15.416	15.000	15.1455	15.0446	15.0124

Table 7 Final normalized value considering all the examples

Category	Best Weight				Mean Weight				Coefficient Variation			
Algorithms	CPA	BBO	TLBO	PSO	CPA	BBO	TLBO	PSO	CPA	BBO	TLBO	PSO
Standard	2.3808	1.3384	2.2873	2.5268	5.1763	1.6296	2.7704	2.9649	10.0650	3.2017	5.5043	5.1980
Gauss-21	12.9325	4.0391	11.8745	20.3324	13.1234	7.2373	5.2926	16.4288	10.1608	7.5290	5.1686	9.3392
Gauss -22	9.3225	3.6766	11.3371	24.4205	7.6491	3.7187	15.1475	10.7190	8.8685	4.0723	11.1113	8.3026
Gauss-23	11.2813	9.6775	7.5943	9.7421	4.4503	7.2093	19.8534	14.5355	6.3742	6.2452	11.5849	9.0385
Libovitch-31	13.3113	8.9426	13.1524	7.2388	7.4568	5.9088	9.7636	11.2511	9.1112	9.3391	6.5925	6.8157
Libovitch-32	11.1417	7.0936	10.0278	6.4603	10.9432	6.3234	12.5822	4.4224	6.1308	6.7106	17.3245	4.9127
Libovitch-33	14.0045	4.6596	7.4063	3.8716	29.6306	19.1262	8.7122	2.9498	25.2973	21.6032	6.6617	2.1503
Piecewise -41	7.1307	42.7756	8.6149	5.4296	11.2780	10.0685	3.8687	29.2985	11.0660	11.1620	5.5092	45.7274
Piecewise -42	9.5605	10.8567	19.2828	9.1606	5.3310	16.8516	5.8511	4.7483	5.2871	8.7748	7.0213	7.4011
Piecewise -43	8.9342	6.9403	8.4226	10.8173	4.9613	21.9266	16.1582	2.6818	7.6391	21.3622	23.5215	1.1145

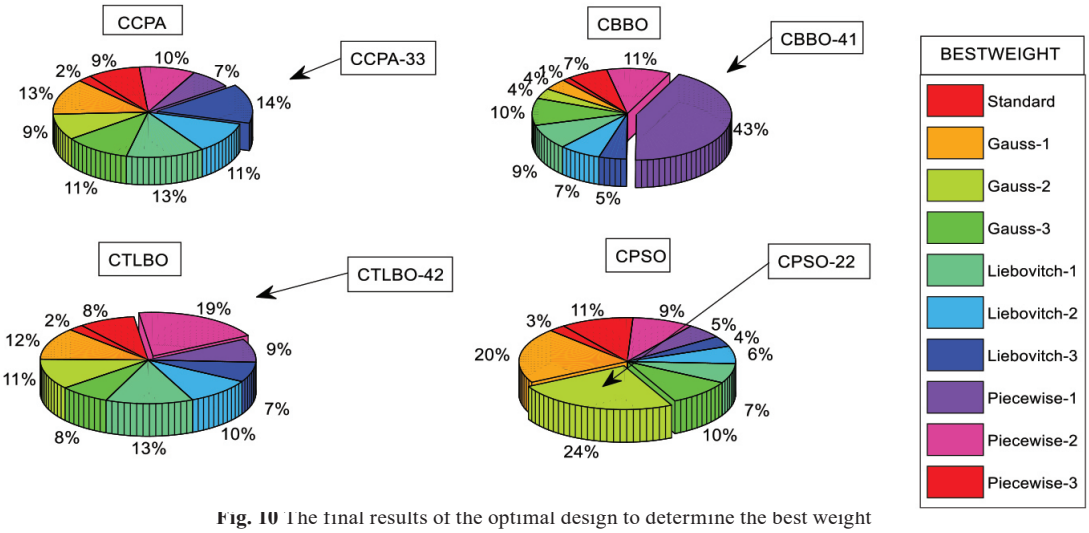

Fig. 10 The final results of the optimal design to determine the best weight

to piecewise chaos map with third scenario and the particle swarm optimization belongs to the Gaussian chaos map with the first scenario. For quick access to the best average information, the pie charts of each of the chaos meta-heuristic algorithms are shown in Fig. 11.

Optimal design for determining the best coefficient of variation for the cyclical parthenogenesis algorithm belonging to the Liebovitch chaos map with the third scenario, the biogeography-based optimization belonging to the Liebovitch chaos map with the third scenario, the teaching-learning-based optimization belonging to the Piecewise chaos map with the third scenario, the particle swarm optimization belongs to the Piecewise chaos map with the first scenario. For quick access to the optimal coefficient of variation information, the pie chart of each of the chaos meta-heuristic algorithms is shown in Fig. 12.

Finally, it should be mentioned that the method of this study can also be applied to other metaheuristics optimization problems, in [46–49].

7 Conclusions

Some of the considerable results in this research are as follows:

- In most cases, the embedded chaotic map in meta-heuristic algorithms has created a significant improvement compared to the standard mode. The main reason can be the effect of chaos maps in escaping local optimization and preventing premature convergence.
- Chaos functions for optimization problems based on frequency constraints and shape variables have been significantly improved. Comparison of the results of the chaos functions with the standard value confirms this.
- In Scenarios 1 and 2, the chaos maps have replaced the exploration and exploitation steps, respectively. Based on these operations, it can be concluded:
- The cyclical parthenogenesis algorithm uses the chaos map for both exploration and exploitation stages. The biogeography-based optimization uses the chaos map

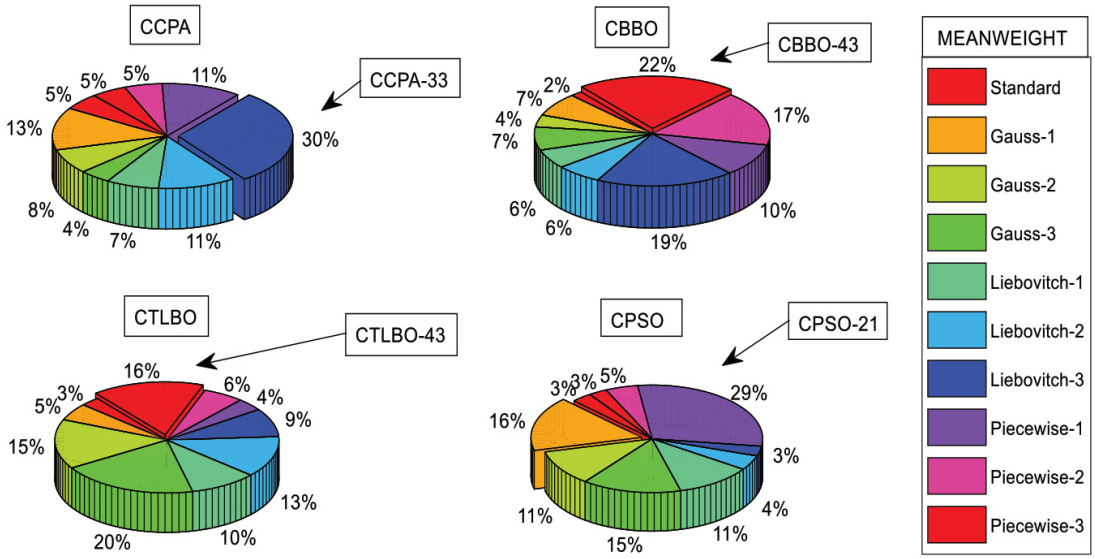

Fig. 11 The final results of the optimal design to determine the best mean

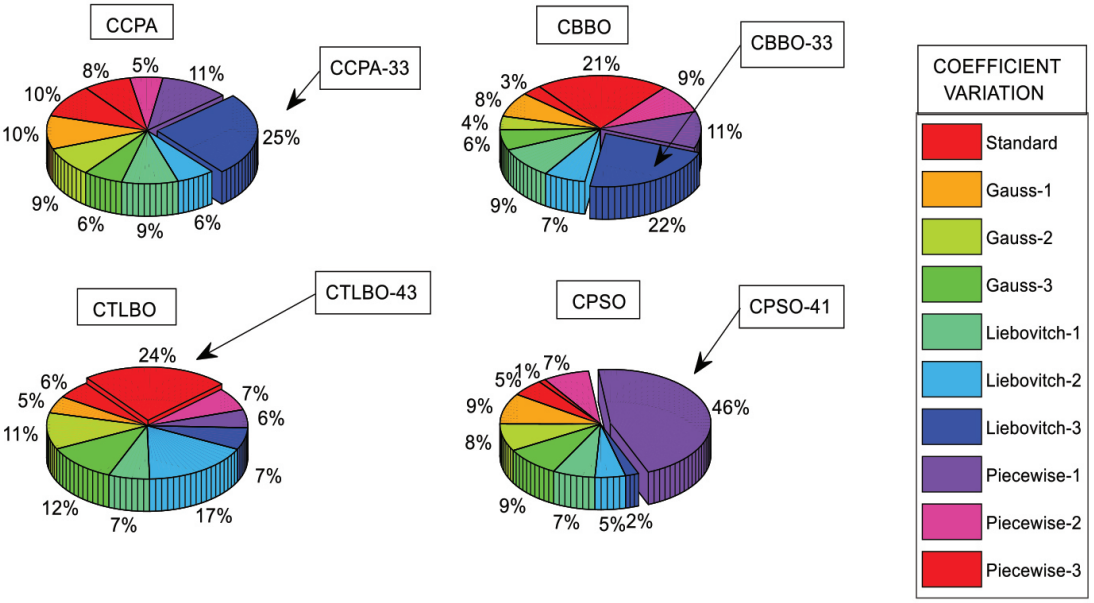

Fig. 12 The final results of the optimal design to determine the best coefficient of variation

in the exploration phase. Teaching-learning-based optimization and particle swarm optimization have both used chaotic maps for the exploitation stage.

- Using the chaos maps, determining the regulatory parameters of algorithms and sensitivity analysis, is significantly removed. In fact, selecting the starting sentence in chaos maps replaces complex settings. It should be noted that in most cases it is more difficult to find the appropriate tuning parameters of each algorithm than self-optimization. Therefore, by using chaos functions, complex engineering problems such as shape optimization can be solved without having to find parameters.
- To evaluate the stability, reliability and robust of the responses, the coefficient of variation, which is the dimensionless state of standard deviation, has been used.
- To select the initiator sentence in the series of chaos maps, before the main iterations, perform several initial iterations and select the appropriate starter sentence to improve the results by leaps and bounds.
- Among the chaos functions investigated, the Piecewise map with Scenarios 1 and 2 has provided the best results for the optimal weight.

References

[1] Kaveh, A. "Advances in Metaheuristic Algorithms for Optimal Design of Structures", 3rd ed., Springer, Cham, Switzerland, 2021. https://doi.org/10.1007/978-3-319-05549-7

[2] Holland, J. H. "Adaptation in Natural and Artificial Systems: An Introductory Analysis with Applications to Biology, Control, and Artificial Intelligence", MIT Press, Ann Arbor, MI, USA, 1975.

[3] Rajeev, S., Krishnamoorthy, C. S. "Discrete optimization of structures using genetic algorithms", Journal of Structural Engineering, 118(5), pp. 1233–1250, 1992. https://doi.org/10.1061/(ASCE)0733-9445(1992)118:5(1233)

[4] Schwefel, H.-P. "Evolutions Strategy and Numerical Optimization", PhD Thesis, Technical University Berlin, 1975.

[5] Price, K. V., Storn, R. M. "Differential Evolution: A Practical Approach to Global Optimization", Springer, Berlin, Heidelberg, 2005. https://doi.org/10.1007/3-540-31306-0

[6] Kaveh, A., Zolghadr, A. "Cyclical parthenogenesis algorithm: a new metaheuristic algorithm", Advances in Engineering Software, (in press) 2016.

[7] Kennedy, J., Eberhart, R. "Particle swarm optimization", In: Proceedings of ICNN'95 - International Conference on Neural Networks, Perth, WA, Australia, 1995, pp. 1942–1948.

[8] Kaveh, A., Zolghadr, A. "Democratic PSO for truss layout and size optimization with frequency constraints", Computer & Structures, 130, pp. 10–21, 2014. https://doi.org/10.1016/j.compstruc.2013.09.002

[9] Karaboga, D. "An idea based on honey bee swarm for numerical optimization", Erciyes University, Kayseri, Turkey, Rep. TR06, 2005.

[10] Kaveh, A., Bakhshpoori, T. "Optimum design of space trusses using cuckoo search", Iranian Journal of Science and Technology, C1(37), pp. 1–15, 2013.

[11] Dorigo, M., Maniezzo, V., Colorni, A. "Ant System: Optimization by a Colony of Cooperating Agents", IEEE Transactions on Systems, Man, and Cybernetics, Part B: Cybernetics, 26(1), pp. 29–41, 1996. https://doi.org/10.1109/3477.484436

[12] Kaveh, A., Zakian, P. "Improved GWO algorithm for optimal design of truss structures", Engineering with Computers, 34, pp. 685–707, 2018. https://doi.org/10.1007/s00366-017-0567-1

[13] Mirjalili, S., Mirjalili, S. M., Lewis, A. "Grey Wolf Optimizer", Advances in Engineering Software, 69, pp. 46–61, 2014. https://doi.org/10.1016/j.advengsoft.2013.12.007

[14] Mirjalili, S., Lewis, A. "The Whale Optimization Algorithm", Advances in Engineering Software, 95, pp. 51–67, 2016. https://doi.org/10.1016/j.advengsoft.2016.01.008

[15] Kaveh, A., Bakhshpoori, T. "Water Evaporation Optimization: A novel physically inspired optimization algorithm", Computers & Structures, 167, pp. 69–85, 2016. https://doi.org/10.1016/j.compstruc.2016.01.008

[16] Kaveh, A., Bakhshpoori, T. "A novel metaheuristic for continuous structural optimization: Water Evaporation Optimization", Structural Multidisiplinary Optimization, 54, pp. 23–43, 2016. https://doi.org/10.1007/s00158-015-1396-8

[17] Kaveh, A., Talatahari, S. "A novel heuristic optimization method: charged system search", Acta Mechanica, 213, pp. 267–289, 2010. https://doi.org/10.1007/s00707-009-0270-4

[18] Kaveh, A., Mahdavi, V. R. "Colliding bodies optimization: A novel meta-heuristic method", Computers & Structures, 139, pp. 18–27, 2014. https://doi.org/10.1016/j.compstruc.2014.04.005

[19] Kaveh, A., Mahdavi, V. R. "Colliding Bodies Optimization method for optimum discrete design of truss structures", Computer & Structures, 139, pp. 43–53, 2014. https://doi.org/10.1016/j.compstruc.2014.04.006

[20] Kaveh, A., Mahdavi, V. R. "Colliding Bodies Optimization: Extensions and Applications", Springer, Cham, Switzerland, 2015. https://doi.org/10.1007/978-3-319-19659-6

[21] Kaveh, A., Ilchi Ghazaan, M. "A new meta-heuristic algorithm: vibrating particles system", Scientia Iranica, Transaction A, Civil Engineering A, 24(2), pp. 551–66, 2017. https://doi.org/10.24200/sci.2017.2417

[22] Kaveh, A., Ilchi Ghazaan, M. "Vibrating particles system algorithm for truss optimization with multiple natural frequency constraints", Acta Mechanica, 228, pp. 307–322, 2017. https://doi.org/10.1007/s00707-016-1725-z

[23] Kaveh, A., Dadras Eslamlou, A. "A novel meta-heuristic optimization algorithm: thermal exchange optimization", Advances in Engineering Software, 110, pp. 69–84, 2017. https://doi.org/10.1016/j.advengsoft.2017.03.014

[24] Erol, O. K., Eksin, I. "New optimization method: Big Bang–Big Crunch", Advances in Engineering Software, 37, pp. 106–111, 2006. https://doi.org/10.1016/j.advengsoft.2005.04.005

[25] Kaveh, A., Talatahari, S. "Size optimization of space trusses using Big Bang–Big Crunch algorithm", Computer & Structures, 87, pp. 1129–1140, 2009. https://doi.org/10.1016/j.compstruc.2009.04.011

[26] Kaveh, A., Khayatazad, M. "A novel meta-heuristic method: Ray Optimization", Computer & Structures, 112–113, pp. 283–294, 2012. https://doi.org/10.1016/j.compstruc.2012.09.003

[27] Kaveh, A. "Ray optimization algorithm", In: Advances in Metaheuristic Algorithms for Optimal Design of Structures, Springer, Cham, Switzerland, 2014, pp. 237–280. https://doi.org/10.1007/978-3-319-46173-1_8

[28] Alatas, B. "Chaotic harmony search algorithms", Applied Mathematical Computing, 216(9), pp. 2687–2699, 2010. https://doi.org/10.1016/j.amc.2010.03.114

[29] Simon, D. "Biogeography-Based Optimization", IEEE Transactions on Evolutionary Computation, 12(6), pp. 702–713, 2008. https://doi.org/10.1109/TEVC.2008.919004

[30] Rao, R. V., Savsani, V. J., Vakharia, D. P. "Teaching–learning-based optimization: a novel method for constrained mechanical design optimization problems", Computer Aided Design, 43(3), pp. 303–315, 2011. https://doi.org/10.1016/j.cad.2010.12.015

[31] Talatahari, S., Kaveh, A., Sheikholeslami, R. "Chaotic imperialist competitive algorithm for optimum design of truss structures", Structural Multidisciplinary Optimization, 46(3), pp. 355–67, 2012. https://doi.org/10.1007/s00158-011-0754-4

[32] Eusuff, M., Lansey, K., Pasha, F. "Shuffled frog-leaping algorithm: a memetic meta-heuristic for discrete optimization", Engineering Optimization, 38(2), pp. 129–154, 2006. https://doi.org/10.1080/03052150500384759

[33] Peitgen, H.-O., Jürgens, H., Saupe, D. "Chaos and Fractals: New Frontiers of Science", Springer, New York, NY, USA, 2006. https://doi.org/10.1007/978-1-4757-4740-9

[34] Kaveh, A., Sheikholeslami, R., Talatahari, S., Keshvari-Ilkhichi, M. "Chaotic swarming of particles: a new method for size optimization of truss structures", Advances in Engineering Software, 67, pp. 136–47, 2014. https://doi.org/10.1016/j.advengsoft.2013.09.006

[35] Bucolo, M., Caponetto, R., Fortuna, L., Frasca, M., Rizzo, A. "Does chaos work better than noise?", IEEE Circuits and Systems Magazine, 2(3), pp. 4–19, 2002. https://doi.org/10.1109/MCAS.2002.1167624

[36] Erramilli, A., Singh, R., Pruthi, P. "Modeling Packet Traffic with Chaotic Maps", KTH, Stockholm, Sweden, 1994.

[37] Lingyun, W., Mei, Z., Guangming, W., Guang, M. "Truss optimization on shape and sizing with frequency constraints based on genetic algorithm", Computational Mechanics, 35(5), pp. 361–368, 2005. https://doi.org/10.1007/s00466-004-0623-8

[38] Gomes, H. M. "Truss optimization with dynamic constraints using a particle swarm algorithm", Expert Systems with Applications, 38(1), pp. 957–968, 2011. https://doi.org/10.1016/j.eswa.2010.07.086

[39] Lin, J. H., Chen, W. Y., Yu, Y. S. "Structural optimization on geometrical configuration and element sizing with static and dynamic constraints", Computers and Structures, 15(5), pp. 507–515, 1982.

[40] Kaveh, A., Javadi, S. M. "Chaos-based firefly algorithms for optimization of cyclically large-size braced steel domes with multiple frequency constraints", Computers & Structures, 214, pp. 28–39, 2019. https://doi.org/10.1016/j.compstruc.2019.01.006

[41] Kaveh, A., Ilchi Ghazaan, M. "Hybridized Optimization Algorithms for Design of Trusses with Multiple Natural Frequency Constraints", Advances in Engineering Software, 79, pp. 137–147, 2015. https://doi.org/10.1016/j.advengsoft.2014.10.001

[42] Tejani, G. G., Savsani, V. J., Patel, V. K. "Adaptive symbiotic organisms search (SOS) algorithm for structural design optimization", Journal of Computational Design and Engineering, 3(3), pp. 226–249, 2016. https://doi.org/10.1016/j.jcde.2016.02.003

[43] Khatibinia, M., Naseralavi, S. S. "Truss Optimization on Shape and Sizing with Frequency Constraints Based on Orthogonal Multi-Gravitational Search Algorithm", Journal of Sound and Vibration, 333(24), pp. 6349–6369, 2014. https://doi.org/10.1016/j.jsv.2014.07.027

[44] Kaveh, A., Kooshkbaghi, M. "Enhanced Artificial Coronary Circulation System Algorithm for Truss Optimization with Multiple Natural Frequency Constraints", Periodica Polytechnica Civil Engineering, 63(2), pp. 362–376, 2019. https://doi.org/10.3311/PPci.13562

[45] Kaveh, A., Zolghadr, A. "Truss optimization with natural frequency constraints using a hybridized CSS-BBBC algorithm with trap recognition capability", Computers & Structures, 102–103, pp. 14–27, 2012. https://doi.org/10.1016/j.compstruc.2012.03.016

[46] Movahedi Rad, M., Habashneh, M., Lógó, J. "Elasto-Plastic limit analysis of reliability based geometrically nonlinear bi-directional evolutionary topology optimization", Structures, 34, pp. 1720–1733, 2021. https://doi.org/10.1016/j.istruc.2021.08.105

[47] Lógó, J., Movahedi Rad, M., Knabel, J., Tauzowski, P. "Reliability based design of frames with limited residual strain energy capacity", Periodica Polytechnica Civil Engineering, 55(1), pp. 13–20, 2011. https://doi.org/10.3311/pp.ci.2011-1.02

[48] Habashneh, M., Movahedi Rad, M. "Reliability based geometrically nonlinear bi-directional evolutionary structural optimization of elasto-plastic material", Scientific Reports, 12, 5989, 2022. https://doi.org/10.1038/s41598-022-09612-z

[49] Li, Q., Yin, X., Huang, B., Zhang, Y., Xu, S. "Strengthening of the concrete face slabs of dams using sprayable strain-hardening fiber-reinforced cementitious composites", Frontiers of Structural and Civil Engineering, 16, pp. 145–160, 2022. https://doi.org/10.1007/s11709-022-0806-4